NTNU
Norwegian University of
Science and Technology

Evaluation of Kalman filters for estimation of the annular bottomhole pressure during drilling

Thomas Rognmo

Master of Science in Engineering Cybernetics
Submission date: June 2008
Supervisor: Ole Morten Aamo, ITK

Norwegian University of Science and Technology
Department of Engineering Cybernetics

Problem Description

Estimation of the annular pressure at critical locations in the well is crucial for high-precision
pressure control. Certain parameters which are important in order to determine the pressure
profile of the well (in particular the friction factor, bulk modulus and density in the annulus), are
encumbered with high uncertainty and are besides, continuously, but slowly changing. The
objective of the thesis is to employ various Kalman filter designs estimation of the bottomhole pressure
and certain important parameters/slowly varying variables, during drilling.

Topics that should be addressed are:
1) Literature review of the theory of Kalman filters design

2) Design and implement an Extended Kalman filter (EKF) and possibly the Unscented Kalman filter
(UKF) for

a) Estimation of the annulus bottom-hole pressure

b) Esimation of the friction coefficient, bulk modulus and density in the annulus

3) Analyse the performance/robustness of the observer in important cases, in particular:

a) Pipe connection

b) Pump ramp up/down

4) Examine observer performance to unmodeled dynamics by testing the Kalman filter against data sets from Wemod

5) Evaluate performance of the observer against experimental data from Grane.

Summary

During drilling a drill-fluid is pumped through the drill-string and drill-bit. The drill-mud flows back in the well bore and trough a choke-valve at top-side. To avoid uncontrolled influx from the reservoir or lost circulation to the formation; the annulus pressure must be kept within the pressure window between pore pressure and fracture pressure. The bottom-hole pressure measurement is often transfered as pressure pulses through the drill-mud. This gives a slow update rate. Also, during low flows the bottom-hole assembly tool turns itself off, and the measurement is lost. When pressure margins are small; proper control of the annulus pressure is crucial. This requires a good estimate or measurement of the pressure.

To estimate the bottom-hole pressure the Extended Kalman filter and Unscented Kalman filter where evaluated. The filters are based on a process model with the states; stand-pipe pressure, choke differential pressure and bit-flow. The bottom-hole measurement equation consists the unknown parameters; bit-flow, annulus density, well-bore friction and bulk-modulus. These parameters are uncertain and varying and must therefore be estimated to obtain a correct estimate of the annulus pressure. To estimate the parameters the joint-EKF and joint-UKF where designed.

The observability analysis of the linearized state equations showed that the process model is not observable when augmenting the state equations with the parameters; annulus density, well-bore friction and fluid bulk-modulus. To handle this the annulus density was calculated off-line and not included in the augmented model.

During drilling there may be long periods with little excitation from the inputs. The filters where therefore designed to switch between estimated parameters. In the Unscented Kalman filter it is possible to implemented this in one filter, whereas in the Extended Kalman filter; one filter for each parameter vector had to be designed. The Extended Kalman filter and Unscented Kalman filter where compared with data obtained from simulations on the design model. When augmenting the state equations with annulus friction and fluid bulk-modulus; both filters estimated the correct value of the unknown parameters, the bit-flow and bottom-hole pressure. The Unscented Kalman filter showed a faster convergence rate and estimated parameter values closer to the correct value than the Extended Kalman filter.

Based on performance and implementation purposes w.r.t switching between parameters; it was chosen to examine the Unscented Kalman filter further. The tests performed on the Unscented Kalman filter where state and parameter estimation on data sets from the Grane field and simulations against Wemod. A pipe-connection scenario was simulated with Wemod. Annulus friction was estimated during stationary conditions and fluid bulk-modulus was estimated during transients. The filter estimated the correct

bottom-hole pressure for stationary conditions and had some deviations during transients. In the simulation against data sets from Grane; the annulus friction and choke valve constant where estimated during stationary conditions. The filter followed the bottom-hole pressure measurement within an error of one bar.

Preface

This master thesis has been written as part of the Master of Technology program at the Norwegian University of Science and Technology, department of Engineering Cybernetics. My special thanks goes to Professor Ole Morten Ammo at NTNU and Dr. Glenn-Ole Kaasa at StatoilHydro for their guidance during the project and for making this study possible. To Øyvind N. Stamnes for his great willing to help and solve my many questions. Lars Imsland for his help and guidance about Kalman filters. And finaly, to my fellow students and friends; Martin Kivle, Henrik Helgesen, Kjetil Hodne and Helle Lorentzen for great advice and a memorable year.

Thomas Rognmo
Trondheim, June 2008

Contents

Chapter 1

Introduction

1.1 Background

In a drilling operation a drilling fluid is circulated thorough the drill-string and drill-bit. The mud flows outside the drill-string in the annulus transporting cuttings form the well-bore. An important objective during drilling is to ensure that the annulus pressure gradient is constrained within the well fracture pressure and the reservoir pore pressure. Conventional drilling techniques such as over balance drilling involves retaining the bottom-hole pressure well above the reservoir pore pressure; this is done to avoid reservoir influx. OBD helps prevent uncontrolled influx, but decreases production rate due to skin damage on the reservoir rock. It's therefore preferred to keep the annulus pressure as close to the reservoir pore pressure as possible. The annulus pressure gradient must also stay below the formation fracture pressure to avoid damage to the bore hole and lost circulation. Today the annulus pressure gradient is usually controlled by manually by adjusting the top-side choke and also by changing the mud density in the drill string. Changing the pressure by adding heavier or lighter fluids to the well slowly changes the pressure gradient. It must therefore be planned ahead. If the choke valve is controlled manually; it is nearly impossible to react to fast pressure changes. This makes drilling difficult when the drilling window is small. When drilling into deeper and more complex formations; maintaining a constant bottom-hole pressure is essential to avoid severe problems. Many reservoirs are therefore undrillable and new solutions must be implemented to ensure a stable bore-hole pressure. A good measurement or estimate of the annular pressure is crucial for controlling the bottom-hole pressure. The measurement available has a slow and irregular update rate and is not suited for feedback control. To estimate the bottom-hole pressure; unknown variables such as annulus density and annulus friction must also be estimated.

1.2 Description of the drilling process

Figure 1.1 display a schematic of the drilling process. Drill-mud is circulated through the drill-pipe and drill-bit utilizing a mud-pump. The mud flows back through the annulus transporting cuttings from the formation. At top-side a rotating control device closes the well, and the mud flows through a choke-valve.

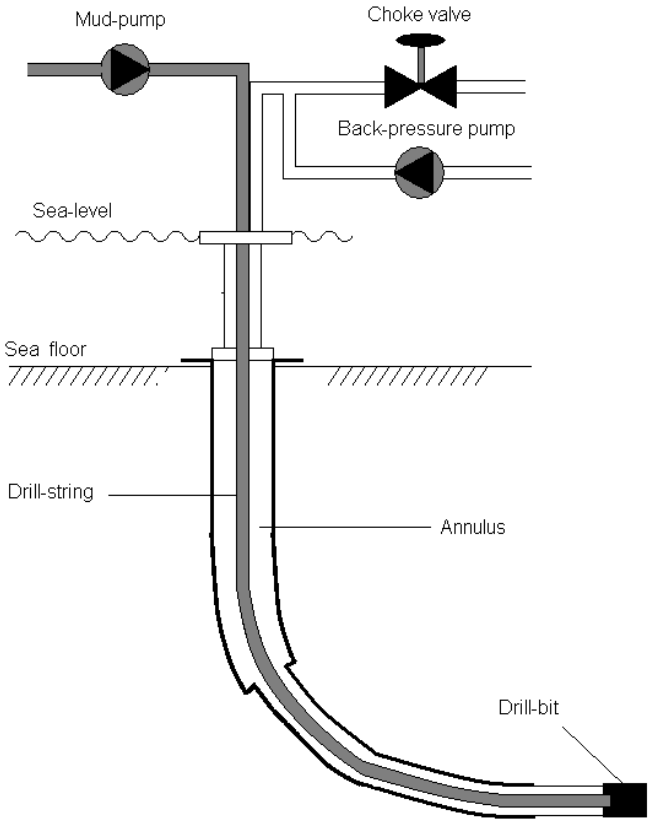

Figure 1.1: Schematic of a drilling-operation

One important objective during drilling is to control the pressure gradient in the well bore. When drilling into a formation; the pressure must be kept below the formation fracture pressure and and above the collapse pressure. In conventional over balance drilling (OBD) the well pressure is kept well above the reservoir pore pressure as the drill-bit enters the reservoir zone. This is to prevent uncontrolled influx from the reservoir and avoid kicks or a blow-out situation. The mud that penetrate the well in the reservoir is called

mud-cake and degrades production. It is therefore desirable to maintain a well pressure as close to the reservoir pressure as possible.

Managed pressure drilling(MPD) is defined as [1] "an adaptive drilling process used to more precisely control the annular pressure profile throughout the well bore." In MPD an objective is to obtain a bottom-hole pressure that do not invite reservoir inflow.

$$p_{coll}(x,t) < p_{res}(x,t) \leq p_a(x,t) < p_{frac}(x,t) \tag{1.1}$$

As seen from equation (1.1); where t is time and x is the position along the well; the pore pressure and fracture pressure gradients in the well-bore will cause a more narrow drilling window as the well becomes deeper. These pressure limits are not known before drilling the well. Also, the reservoir pore pressure may change as the drill-bit enter deeper into the reservoir zone.

1.3 Measurements

The pressure measurements available are stand-pipe pressure p_p, choke-differential pressure p_c and bottom-hole pressure p_a. The latter measurement is often transferred as pressure pulses through the mud along with other measurements. This gives a slow update rate on the pressure measurement. Another problem is that the bottom-hole assembly tool is turned off during low bit-flows and the measurement is lost. Other measurements assumed known are

- True vertical depth (TVD)
- Well length
- Choke valve input
- Mud-pump flow
- Back-pressure pump flow
- Equivalent circulating density (ECD)

1.4 Pressure control

The annulus pressure gradient is mainly determined by the hydrostatic height, friction in the well-bore and the choke valve opening. All these three variable may be utilized for controlling the annulus pressure profile. Density has the largest influence on annulus pressure and may be altered by changing the composition of the drill-mud. The flow rate generated by the mud-pump

[1] Defined by the International Association of Drilling Contractors

causes a pressure loss due to friction in the well bore. This pressure loss may lead to a challenge in controlling the pressure as the pump speeds are altered. In normal operation the pump speed is maintained constant and pressure is controlled with the choke valve. For small choke valve openings the valve may be clogged by cuttings from the well. In some installations a back-pressure pump is therefore included to supply additional pressure when needed. Typical pressure disturbances are variations in reservoir pore pressure, drill-string movements and stopping and starting mud-pump circulation. The latter situation is performed during pipe-connections; i.e the mud-pump is ramped down, a new drill string is connected, the mud-pump is ramped up again and drilling is resumed. In this situation the pressure variations may be large and the back-pressure pump can by utilized to supply additional pressure.

To ensure satisfactory pressure management in the well bore; a controller based on feedback from the bottom-hole pressure should be utilized. For papers related to annulus pressure control see for instance [17] and [16]. In [17] a linear MPC and a PID is utilized for controlling the pressure and in [16]; an $\mathcal{H}_\infty$-controller and a PID is compared for controlling the pressure based on a top-side pressure measurement. When the controller is based on feedback from the top-side measurement; the annulus friction and density is not taken into consideration in the controller. However; the controller dampen the effect of pressure disturbances to some degree.

1.5 Pressure estimation

To properly control the bottom-hole pressure; a measurement or estimate of the bottom-hole pressure is needed. Such a measurement exists, but the signal has a very slow bit-rate and is lost during low flows; for instance during a pipe-connection. This makes the measurement a poor choice for control. In order to estimate the bottom-hole pressure there are a number of unknown variables that must be determined. As mentioned; the main contribution to the bottom-hole pressure is annulus density and annulus friction. To obtain the dynamics of the system; the pressure pulses and flow dynamics must also be taken into consideration. The drill-string density can be measured, but due to cuttings and possible influx from the reservoir; the annulus density is unknown. The well-bore friction is also combined with great uncertainty.

For other sources on bottom-hole pressure estimation; see for instance [18]. Here an adaptive observer is designed for estimating unknown well parameters and the bottom-hole pressure.

1.6 Scope and emphasis

In this report the possibility of estimating the bottom-hole pressure utilizing a Kalman filter is examined. The Kalman filter is based on the fluid model derived in the internal document [12]. The filters evaluated are the Extended Kalman filter (EKF) and the Unscented Kalman filter (UKF). First an analysis based on which parameters to estimate is performed. Different EKF and UKF filters are designed based on the observability and limitations of the filter and input excitation. The primary objective is to estimate the bottom-hole pressure based on the stand-pipe pressure and choke differential pressure measurements. The UKF is then tested against simulations in Wemod and data sets from the Grane field.

Chapter 2

Kalman filter theory

This sections describes the discrete Kalman filter and how it can be utilized for estimating states, disturbances and parameters of a set of non-linear difference equations.

2.1 Discretization of state equations

In this report the discrete Kalman filter is considered. This requires a discrete representation of the continuous differential equations. Let the nonlinear differential equations be described as

$$\begin{aligned} \dot{x}(t) &= f(x,u) + w(t) \\ z(t) &= h(x) + v(t) \end{aligned} \tag{2.1}$$

where $x \in \mathbb{R}^n$ represents the unobserved states, $z \in \mathbb{R}^m$ denote the observed variables and $u \in \mathbb{R}^l$ is the controlled variable. w and v are white noise processes with covariance

$$\begin{aligned} E[w(t+\tau)w(\tau)] &= Q(t)\delta(\tau) \\ E[v(t+\tau)v(\tau)] &= R(t)\delta(\tau) \\ E[v(t)w(t+\tau)] &= 0 \quad \forall\tau \end{aligned} \tag{2.2}$$

Calculation of the Kalman filter can be performed by considering a discrete form of equation (2.1), or by utilizing the continuous state equations with discrete measurements.

The nonlinear differential equations (2.1) can be represented in a discrete form by applying explicit Euler

$$\begin{aligned} x_{k+1} &= x_k + hf(x_k, u_k) + hw_k \\ z_k &= h(k) + hv_k \end{aligned} \tag{2.3}$$

with covariance matrix

$$Q_k = Q/h$$

where h is the step For numeric stability the method requires

$$h \leq -2/\lambda_{min}$$

where λ_{min} is the smallest eigenvalue in the state equations. If the continuous differential equations are stiff there may be problems with stability, since this require a very small step size.

2.2 Mean square estimation

[1] Consider the estimation of a random vector X given the measurement Z. The objective is to estimate $X(Z)$ so that the error

$$\tilde{X} = X - \hat{X}$$

is minimized. We define the cost function as the mean square error

$$J = E\left\{(X - \hat{X})(X - \hat{X})^T\right\} \tag{2.4}$$

and restrict the estimate $X(Z)$ to be a linear combination of the measurements[2].

$$X(Z) = AZ + b \tag{2.5}$$

Substituting this into the cost function results in

$$\begin{aligned}
J &= E\left\{(X - \hat{X})(X - \hat{X})^T\right\} = trace\left[E\left\{(X - \hat{X})(X - \hat{X})^T\right\}\right] \\
&= trace\left[E\left\{(X - AZ - b)(X - AZ - b)^T\right\}\right] \\
&= trace\left\{\left[(X - \bar{X}) - (AZ + b - \bar{X})\right]\left[(X - \bar{X}) - (AZ + b - \bar{X})\right]\right\} \\
&= trace\left[P_{xx} + A(P_{zz} + \bar{Z}\bar{Z})A^T + (b - \bar{X})(b - \bar{X})^T + 2A\bar{Z}(b - \bar{X})^T - 2AP_{xz}\right]
\end{aligned}$$

where P_{zx} is the cross covariance between Z and X. To find the optimal values this equation is differentiated with respect to A and b

$$\begin{aligned}
\frac{\partial J}{\partial b} &= 2(b - \bar{X}) + 2A\bar{Z} = 0 \\
\frac{\partial J}{\partial A} &= 2A(P_z + \bar{Z}\bar{Z}^T) - 2P_{xz} + 2(b - \bar{X})\bar{Z}^T = 0
\end{aligned}$$

solving for A and b

$$\begin{aligned}
b &= \bar{X} - A\bar{Z} \\
A &= P_{xz}P_{zz}^{-1}
\end{aligned}$$

[1] Theory from the following sections is captured from [10], [6] and [13]

[2] No assumptions are made on the relation between Z and $\hat{X}$. The results are valid for any possible nonlinear relation between measurement and unknown [13, chapter 1]

Inserting into equation (2.5) results in the linear mean square estimate

$$\hat{X}_{LMS} = \bar{X} + P_{xz}P_{zz}^{-1}(Z - \bar{Z}) \tag{2.6}$$

Obtaining P_{zz}, P_{xz} and $\bar{Z}$ is not a trivial task. It requires knowing the conditional probability density function of X given Z as it is transformed through a function; possibly nonlinear. If the relationship between X and Z is a linear state space system; equation (2.6) simplifies to the Kalman filter equations.

2.2.1 Discrete Kalman filter

In the general form the discrete Kalman filter is utilized for estimation of the states in the linear stochastic difference equations

$$\begin{aligned} x_{k+1} &= A_k x_k + B_k u_k + w_k \\ y_k &= C_k x_k + v_k \end{aligned} \tag{2.7}$$

where $x \in \mathbb{R}^n$ represents the unobserved states, $y \in \mathbb{R}^m$ denote the observed variables and $u \in \mathbb{R}^l$ is the controlled variable. w_k and v_k are white noise processes with covariance

$$\begin{aligned} E[w_k w_i] &= Q_k \delta_{ki} \\ E[v_k v_i] &= R_k \delta_{ki} \\ E[w_k w_i] &= 0 \end{aligned} \tag{2.8}$$

$\hat{x}_k^-$ is defined as the a priori state estimate calculated at the previous step $k-1$, and $\hat{x}_k$ is the posteriori state estimate at step k. The a priori and posteriori error estimate is defined as

$$\begin{aligned} e_k^- &\triangleq x_k - \hat{x}_k^- \\ e_k &\triangleq x_k - \hat{x}_k \end{aligned}$$

and the a priori and posteriori error covariance can then be defined as

$$\begin{aligned} P_k^- &= E[e_k^- e_k^{-T}] \\ P_k &= E[e_k e_k^T] \end{aligned}$$

Filtering of the states and covariance is based on a trade-off between the a priori estimate and the current measurement

$$\begin{aligned} \hat{x}_k &= \hat{x}_k^- + K_k(y_k - C_k \hat{x}_k^-) \\ P_k &= (I - K_k C_k) \end{aligned} \tag{2.9}$$

where the Kalman gain K_k is determined by

$$K_k = P_k^- C_k^T (C_k P_k^- C_k^T + R_k)^{-1}$$

Based on the new estimate given in equation (2.9); the predicted states and covariance can be calculated as

$$\begin{aligned} \hat{x}_{k+1} &= A_k \hat{x}_k + B_k u_k \\ P_{k+1} &= A_k P_k A_k^T + R_k \end{aligned}$$

2.3 The extended Kalman filter

For systems where the difference equations are nonlinear; the filter in section 2.2.1 might not be adequate. The extended Kalman filter solves this by approximating the time and measurement update around the current estimate.

A set of nonlinear difference equations can be described as

$$\begin{aligned} x_{k+1} &= f(x_k, u_k) + w_k \\ z_k &= h_k(x_k) + v_k \end{aligned} \tag{2.10}$$

where w_k and v_k are white noise processes with expectation and covariance as described in (2.8).

2.3.1 Time and measurement update equations

The exact time updates for the first two moments of x_k and z_k are

$$\begin{aligned} \hat{x}_k^- &= E[f(x_k, u_k) + w_k] \\ K_k &= P_{xz} P_{\bar{y}\bar{y}}^{-1} \\ \hat{y}_k^- &= E[h(x_k^-) + v_k] \end{aligned}$$

These equations are in general not possible to obtain, since it requires knowing the first two moments of x_k and z_k after they have undergone a nonlinear transformation. Instead; the discrete measurement update and time update are approximated by a first order Taylor expansion around the a priori estimate. We denote the Jacobian's as

$$F_{x_k} = \left.\frac{\partial f(x, u_k)}{\partial x}\right|_{x=\hat{x}_k^-} \qquad H_{x_k} = \left.\frac{\partial h(x)}{\partial x}\right|_{x=\hat{x}_k} \tag{2.11}$$

The Kalman filter measurement updates are then given by

$$\begin{aligned} \hat{x}_k &= \hat{x}_k^- + K_k[z_k - h(x_k^-)] \\ K_k &= P_k^- H_{x_k}^T [H_{x_k} P_k^- H_{x_k}^T + R]^{-1} \\ P_k &= [I - K_k H_{x_k}] P_k^- \end{aligned} \tag{2.12}$$

and the predicted time update is calculated as

$$\begin{aligned} x_{k+1} &= f(\hat{x}_k, u_k) \\ P_{k+1} &= F_{x_k} P_k F_{x_k}^T + Q_k \end{aligned} \tag{2.13}$$

2.4 The unscented Kalman filter

[3] When the Kalman filter estimates the measurement and time update it utilizes the mean and covariance of x_k and z_k. When these variables are transformed through a nonlinear function

$$y = f(x)$$

the precise statistics of y can only be calculated if the conditional probability density function $fx|z$ is known. A Taylor expansion around $\bar{x}$ is given by

$$f(x) = f(\bar{x}+\delta x) = f(\bar{x}) + \nabla f \delta x + \frac{1}{2}\nabla^2 f \delta x^2 + \frac{1}{3!} f \nabla^3 f \delta x^3 + \frac{1}{4!}\nabla^4 f \delta x^4 + \dots$$

where δx is Gaussian white noise with zero mean. It can be shown that the mean and covariance of this Taylor expansion are

$$\begin{aligned} \bar{y} &= f(\bar{x}) + \frac{1}{2}\nabla^2 f P_{xx} + \frac{1}{4}E[\delta x^4] + \dots \\ P_{yy} &= \nabla f P_{xx} (\nabla f)^T + \frac{1}{2\times 4!}\nabla^2 f \left(E[\delta x^4] - E[\delta x^2 P_{yy}] - E[P_{yy}\delta x^2] + P_{yy}^2\right)\left(\nabla^2 f\right)^T \\ &\quad \frac{1}{3!} f E[\delta x^4]\left(\nabla^4 f\right)^T + \dots \end{aligned} \tag{2.14}$$

An approximation to the mean and covariance is found by linearizing around $\bar{x}$

$$\begin{aligned} \bar{y} &= f(\bar{x}) \\ P_{yy} &= \nabla f P_{xx} (\nabla f) \end{aligned}$$

and utilizing this mean and covariance for filtering and prediction. As seen from the above equations; this will only give a satisfactory result if the higher order terms are neglectable.

2.4.1 Unscented transform

The UKF utilizes the unscented transform (UT) for calculating the mean and covariance of a random variable propagated through a nonlinear function. To determine the first two moments of y; a set of $2n+1$ sigma-points with sample mean $\bar{x}$ and sample covariance P_{xx} are transformed through the nonlinear function. The points and are selected according to

$$\begin{aligned} \mathcal{X}_0 &= \bar{x} \\ \mathcal{X}_i &= \bar{x} + \left(\sqrt{(n+\lambda)P_{xx}}\right)_i \quad i = 1, \dots n \\ \mathcal{X}_i &= \bar{x} - \left(\sqrt{(n+\lambda)P_{xx}}\right)_i \quad i = n+1, \dots 2n \end{aligned} \tag{2.15}$$

[3] The theory in this section is collected from [1], [5] and[7]

where n is the dimension of the state vector x, $\left(\sqrt{n+\lambda}P_{xx}\right)_i$ is the ith column or row of the matrix square root, and λ is a scaling parameter

$$\lambda = \alpha^2(n+\kappa) + n$$

where α determines the spread of the sigma-points around $\bar{x}$; set to a small value (10^{-3}), β include information about the distribution of x; $\beta = 2$ for a Gaussian distribution, and κ is a tuning parameter; usually set to zero[7]. The weights associated with each sigma point is calculated as

$$\begin{aligned}
W_{m_0} &= \lambda/(n+\lambda); \\
W_{c_0} &= \lambda/(n+\lambda) + 1 - \alpha^2 + \beta; \\
W_{m_i} &= 1/(2(\lambda+n)); \\
W_{c_i} &= W_{m_i} \quad \forall i \geq 1
\end{aligned}$$

Each sigma-point is transformed through the nonlinear function

$$\mathcal{Y}_i = f(\mathcal{X}_i)$$

and the transformed points are utilized for determining the new mean and covariance according to

$$\bar{y} = \sum_{i=0}^{2n} W_i \mathcal{Y}_i$$

$$P_{yy} = \sum_{i=0}^{2n} W_i \left(\mathcal{Y}_i - \bar{y}\right)\left(\mathcal{Y}_i - \bar{y}\right)^T$$

Because the mean and covariance of x is calculated to the second order; the transformed mean and covariance are at least accurate to the second order. It is possible to tune the filter so that a higher order is obtained. In comparison; the EKF calculates the covariance to the same second order and the mean to the first order.

2.4.2 Unscented transform and the unscented Kalman filter

The UT can easily be incorporated into the Kalman filter. Considering the state and measurement equations (2.10); the UT can be employed in the Kalman filter as

1. Predict states $\hat{x}_k^-$ and covariance P_{xx}^- by transforming sigma-points $\mathcal{X}_i$ through state equations $f(x_k, u_k) + hw_k$

2. Predict expected measurements $\hat{y}_k^-$ and covariance $P_{\bar{y}\bar{y}}$ by transforming the sigma-points $\mathcal{X}_i$ through the measurement equation $h(x) + hv_k$

3. Calculate cross-covariance P_{xy}

$$P_{xy} = \sum_{i=0}^{2n} W_i \left(\mathcal{X}_i - \bar{x}_k^-\right)\left(\mathcal{Y}_i - \bar{y}^-\right)^T$$

4. Determine Kalman gain and filtrate estimated state and covariance

$$\begin{aligned} K_k &= P_{yy}P_{xy}^{-1} \\ x_k^- &= \hat{x}_k^- + K_k(y_k - \hat{y}_k^-) \\ P_k &= P_k^- - K_k P_{\bar{y}\bar{y}} K_k^T \end{aligned}$$

2.5 Augmentation of the state-space model

To be able to estimate parameters and disturbances utilizing the Kalman filter; the unknown variables are modeled as additional states in the process model. If we consider parameter estimation in the linear state space equations

$$\begin{aligned} x_{k+1} &= Ax_k + Bu + B_d d_k + B_b b_k + w_k^x \\ z_k &= Hx_k + v_k^x \end{aligned}$$

where d_k and b_k is unknown disturbances and bias. To estimate the parameters and unknown parameters this model can be augmented as

$$\begin{aligned} x_{k+1} &= A(\theta)x_k + B(\theta)u_k + B(\theta)d_k + B(\theta)b_k + w_k^x \\ d_{k+1} &= d_k + w_k^d \\ b_{k+1} &= b_k + w_k^b \\ \theta_{k+1} &= \theta_k + w_k^\theta \\ z_k &= H(\theta)x_k + v_k \end{aligned} \tag{2.16}$$

where w_k^x, w_k^d, w_k^b and w_k^θ are white noise processes with covariances

$$\begin{aligned} E[w_k^x w_i^{xT}] &= Q_k^x \delta_{ki} \\ E[w_k^d w_i^{dT}] &= Q_k^d \delta_{ki} \\ E[w_k^b w_i^{bT}] &= Q_k^b \delta_{ki} \\ E[w_k^\theta w_i^{\theta T}] &= Q_k^\theta \delta_{ki} \end{aligned}$$

The state vectors for equation (2.16) can now be defined

$$\chi_k = \begin{pmatrix} x_k \\ d_k \\ b_k \\ \theta \end{pmatrix} \quad w_k = \begin{pmatrix} w_k^x \\ w_k^d \\ w_k^b \\ w_k^\theta \end{pmatrix} \quad u_k = \begin{pmatrix} u_k \\ 0 \\ 0 \\ 0 \end{pmatrix}$$

with state matrices

$$F(\theta) = \begin{pmatrix} A(\theta) & B_d(\theta) & B_b(\theta) & 0 \\ 0 & I^r & 0 & 0 \\ 0 & 0 & I^s & 0 \\ 0 & 0 & 0 & I^t \end{pmatrix} \quad G(\theta) = \begin{pmatrix} B_u(\theta) \\ 0 \\ 0 \\ 0 \end{pmatrix}$$

If an EKF is used for estimation; the new state equations may be linearized w.r.t $F(\theta)$ and $G(\theta)$ to get the full augmented state space model

$$f(\chi_k, u_k) = F(\theta)\chi_k + G(\theta)u_k$$
$$h(\chi_k) = H(\chi)x_k$$

$$\bar{F}_k = \frac{\partial f(\chi_k, u_k)}{\partial \chi^T} = \begin{pmatrix} F_k(\theta) & \frac{\partial}{\partial \theta^T}\left[F(\theta)\chi_k + G(\theta)u_k\right] \\ \mathbf{0} & I^{r+s+t} \end{pmatrix}_{\chi_k=\hat{\chi}_k, \theta_k=\hat{\theta}_k} \tag{2.17}$$

$$\bar{H}_k = \frac{\partial h(\chi_k^-)}{\chi_k^T} = \begin{pmatrix} H(\theta) & \frac{\partial}{\theta_k^T}\left[H(\theta_k)\chi_k\right] \end{pmatrix}_{\chi_k=\hat{\chi}_k^-, \theta_k=\theta_k^-} \tag{2.18}$$

The discrete state augmentation can be applied to both extended and unscented Kalman filters, the latter does not require the state equation Jacobian's derived above; instead the filter is applied to the augmented nonlinear system.

Chapter 3

Dynamic fluid model

In this chapter the process model utilized for Kalman filter design is derived. The equations where originally deduced in the internal document [12]. It is assumed that the fluid mud can be considered as a one phase hydraulic fluid. The the momentum equation and equation of continuity was applied to the schematic in figure 3.1. Temperatures are assumed to be slowly varying and are treated as constant. The energy equation is therefore not considered. As we can see from the figure; the drill-string and annulus is divided into two separate control volumes connected through the drill-bit. The mud pump is connected to the drill-string at top-side, and a choke valve and a back-pressure pump is connected at top-side on the annulus side.

3.1 Deduction of three state fluid model

The assumptions made when deriving the model are as follows

- Turbulent flow; i.e $Re > 2300$
- One dimensional flow along the flow path.
- Homogeneous cross section area conditions.
- Constant density in the momentum equation.
- Temperature changes are negligible and are treated as constant.

3.1.1 Equation of state

Viscosity μ as a function of temperature T and pressure p is treated as a constant. This is based on the assumption of a slowly varying temperature, and the fact that μ only changes slightly with p.

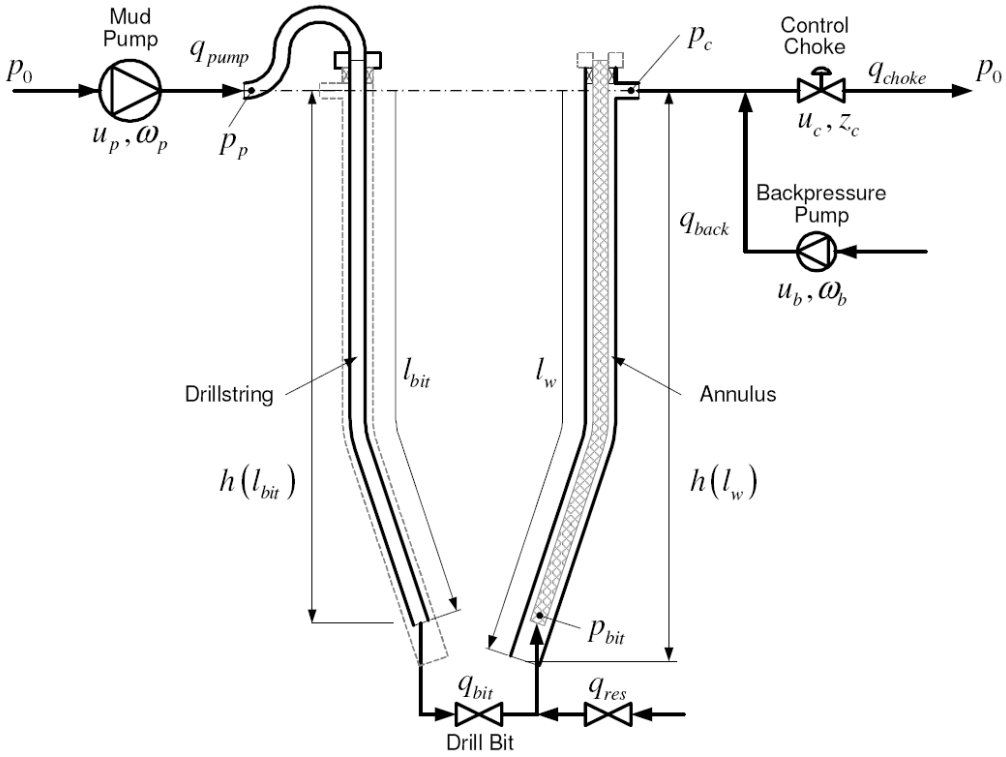

Figure 3.1: Schematic of drilling-configuration

Mud density ρ is given by $\rho = \rho(p, T)$. Since the temperature and pressure changes in a liquid have a small effect on the density, it may be approximated

$$\rho(p,T) \approx \rho_0 + \left.\frac{\partial \rho}{\partial p}\right|_{T_0} (p - p_0) + \left.\frac{\partial \rho}{\partial T}\right|_{p_0} (T - T_0) \tag{3.1}$$

According to the assumptions above; temperature changes have negligible effects on the fluid and are therefore omitted. The bulk modulus; which can be viewed as a measure of liquid compressibility; is defined as

$$\beta \triangleq \rho_0 \left.\frac{\partial p}{\partial \rho}\right|_{T_0} = -V_0 \left.\frac{\partial p}{\partial V}\right|_{T_0}$$

Inserting this into equation (3.1) gives

$$\rho = \rho_0 + \frac{\rho_0}{\beta}(p - p_0) \tag{3.2}$$

3.1.2 Control volume

According to the principle of mass conservation the mass of a material volume V_m is constant

$$m = \iiint_{V_m(t)} \rho dV \Rightarrow \frac{D}{Dt} \iiint_V \rho dV = 0 \tag{3.3}$$

If we assume that ρ is the same all over the control volume and consider Reynolds' transport theorem [4, chapter 10]

$$\frac{d}{dt} \iiint_{V_c} \rho dV = \underbrace{\frac{D}{Dt} \iiint_{V_c} \rho dV}_{equals\ zero,\ see\ (3.3)} - \iint_{\partial V_c} \rho \cdot \vec{n} dA \tag{3.4}$$

Equation (3.4) states that the change in mass equals the net flow into the control volume. Denoting $w = \rho q$ and differentiating the left side of equation (3.4) results in

$$V_c \frac{d\rho}{dt} + \rho \frac{dV_c}{dt} = \sum_i \rho q_{in,i} - \sum_j \rho q_{out,j} \tag{3.5}$$

Inserting the bulk modulus

$$\frac{d\rho}{\rho} = \frac{dp}{\beta} \Rightarrow \dot{\rho} = \frac{\rho}{\beta} \dot{p}$$

into equation (3.5) gives the mass balance for the control volume V_c

$$\frac{V_c}{\beta} \dot{p} + \dot{V}_c = \sum_i q_{in,i} - \sum_j q_{out,j} \tag{3.6}$$

3.1.3 The momentum equation

Navier-Stokes for one dimensional flow is given by

$$\rho \frac{dv}{dt} = -\frac{\partial p}{\partial x} - \frac{1}{A} \frac{\partial F}{\partial x} + \rho g \frac{\partial h}{\partial x} \tag{3.7}$$

where A is the cross section of the pipe, F accounts for friction losses, x is the position along the fluid path and v is the velocity in the x direction.

Friction losses

The friction term in equation (3.7) accounts for all frictional losses and is modeled as

$$\frac{\partial F}{\partial x} = S\tau_w, \quad \tau_w = f \frac{1}{4} \frac{\rho}{2} v^2$$

where S is the pipe perimeter, τ_w is the wall shear stress, and f is the friction factor. For minor losses such as restrictions and pipe bends the friction is given by

$$p_1 - p_2 = K\frac{\rho}{2}v^2$$

If the velocity v is replaced by $v = q/A(x)$ the total friction gradient is

$$\frac{\partial F}{\partial x} = \frac{1}{4}fS(x)\frac{\rho}{2}\left(\frac{q}{A(x)}\right)^2 + \frac{\partial K}{\partial x}A(x)\frac{\rho}{2}\left(\frac{q}{A(x)}\right)^2 \tag{3.8}$$

where $\partial K/\partial x$ is the minor loss gradient along the flow path.

3.1.4 Flow dynamics

To simplify the flow dynamics the flow rate $\bar{q} = A\bar{v}$ and density $\rho = \rho_0$ is assumed constant along the flow path

$$\frac{\rho_0}{A(x)}dx\frac{d\bar{q}}{dt} = -\frac{\partial p}{\partial x} - \frac{1}{A(x)}\frac{\partial F}{\partial x}dx + \rho_0 g\frac{\partial h}{\partial x} \tag{3.9}$$

Integrating along x gives

$$\begin{gathered}\int_0^l \frac{\rho_0}{A(x)}dx\frac{d\bar{q}}{dt} = -\int_0^l \frac{\partial p}{\partial x}dx - \int_0^l \frac{1}{A(x)}\frac{\partial F}{\partial x}dx + \int_0^l \rho g\frac{\partial h}{\partial x}dx \\ \Downarrow \\ \frac{\rho_0 l}{\bar{A}}\frac{d\bar{q}}{dt} = p(0) - p(l) - \left(B_0(l) - fB_1(l)\right)\frac{\rho_0}{2}\bar{q}^2 + \rho_0 g(h(l) - h(0)),\end{gathered} \tag{3.10}$$

where $B_0(l)$ and $B_1(l)$ are defined as

$$B_0(l) \triangleq \int_0^l \frac{\partial K}{\partial x}\frac{1}{A(x)^2}dx \quad B_1 \triangleq \int_0^l \frac{1}{4}\frac{S(x)}{A(x)^3}dx \tag{3.11}$$

and $\bar{A}$ is

$$\bar{A} \triangleq \frac{1}{l}\int_0^l A(x)dx \tag{3.12}$$

3.1.5 Drill-string dynamics

The only actuator in the drill-string is as mentioned the mud pump. Dynamics in the pump is not considered and the flow is described by q_{pump}.

Drill-string pressure

From the control volume equation (3.6) the pressure dynamics can be described as

$$\frac{V_d}{\beta_d}\dot{p}_p = q_{pump} - q_{bit} \tag{3.13}$$

where p_p is the stand-pipe pressure and $\dot{V}_d = 0$ since the drill string volume is constant between pipe connections.

Drill-string flow

The drill-string flow dynamics can be derived from equation (3.10)

$$\frac{\rho_{d0} L_{dN}}{\bar{A}_d}\dot{q}_d = p_p - p_{bit} - (B_{d0} + f_d B_{d1})\frac{\rho_{d0}}{2}q_d^2 + \rho_{d0} g h_{bit} \tag{3.14}$$

where L_{dN} is the total length of the drill-string, p_{bit} is the pressure at the drill-bit and h_{bit} is the hydrostatic height of the fluid; i.e well depth.

3.1.6 Annulus dynamics

From figure 3.1 we see that actuators on the annulus side include a choke valve and a back-pressure pump. The choke valve is modeled as

$$q_{choke} = AK_c z\sqrt{\frac{2}{\rho_a}\Delta p_c} \tag{3.15}$$

Annulus pressure

Applying equation (3.6) to the annulus control volume results in

$$\frac{V_a}{\beta_a}\dot{p}_c + \dot{V}_a = q_{bit} + q_{res} + q_{res} + q_{back} - q_{choke} \tag{3.16}$$

where q_{res} is reservoir inflow and q_{back} is the back-pressure flow.

3.1.7 Annulus flow

We define $q_a = q_{res} + q_{bit}$ and apply equation (3.10)

$$\frac{\rho_0 l_{bit}}{\bar{A}_a}\dot{q}_a = p_{bit} - p_c - (B_{a0} + f_a B_{a1})\frac{\rho_{a0}}{2}q_a^2 + \rho_{d0} g h_{bit} \tag{3.17}$$

3.1.8 Three state fluid model

From figure 3.1 we see that $q_d = q_{bit}$ and we have that; $q_a = q_{bit} + q_{res}$, where q_{bit} is the flow through the drill-bit. If we combine the drill-string flow dynamics (3.14) and annulus flow dynamics (3.17) the state equations can be derived. For simplification the following definitions are included:

$$M_d \triangleq \frac{\rho_{d0} L_{dN}}{\bar{A}_d} \quad M_a \triangleq \frac{\rho_{a0} l_{bit}}{\bar{A}_a(l_{bit})} \tag{3.18}$$

$$F_d \triangleq (B_{d0} + f_d B_{d1})\frac{\rho_{d0}}{2} \quad F_a \triangleq (B_{a0}(l_{bit}) + f_a B_{a1}(l_{bit}))\frac{\rho_{a0}}{2} \tag{3.19}$$

The final process model is shown in equation (3.20).

$$\begin{aligned}
\frac{V_d}{\beta_d}\dot{p}_p &= q_{pump} - q_{bit} \\
\frac{V_a}{\beta_a}\dot{p}_c &= -\dot{V}_a + q_{bit} + q_{res} + q_{back} - zA_cK_c\sqrt{\frac{2}{\rho_{a0}}(p_c - p_0)} \\
(M_a + M_d)\,\dot{q}_{bit} &= p_p - p_c - F_d q_{bit}^2 - F_a(q_{bit} - q_{res})^2 + (\rho_{d0} - \rho_{a0})gh_{bit}
\end{aligned} \tag{3.20}$$

The annulus pressure can now be described as

$$p_a(l) = p_c + M_a(l)\dot{q}_{bit} + F_a(l)q_{bit}^2 + \rho_{a0}gh(l) \tag{3.21}$$

Chapter 4

Model considerations and analysis

4.1 Parameter identification

In the model described in section 3.1.8 there are several parameters that needs to be determined. These parameters can be divided into time-varying, constant and unknown. It is also distinguished between parameters that can be estimated during stationary conditions and parameters that only can be estimated during transients.

In addition to the pressure measurements p_p and p_c; it is assumed that q_{pump}, q_{back}, z, h_{bit} and l_{bit} are known. The drill-string and annulus volumes may be determined from the well length l_{bit}. Based on off-line measurements of the mud density it is possible to calculate the drill-string density ρ_d. The pump flows can be determined by

$$q_{pump} = N_p V_p 2\pi\omega_p$$
$$\tau_p \dot{\omega}_p = -\omega_p + K_{pump} u_p$$

where ω_p rad/s is the pump rotational speed, N_p is the number of pistons and V_p is the volume per strokes per piston [12]. The choke flow is determined from the valve equation

$$q_{choke} = C_v z \sqrt{\Delta p_c}$$
$$\tau_c \dot{z} = -z + u_c$$

where $z \in (0, 1)$ is the valve opening and 0 is fully closed and 1 is fully open. C_v is the valve constant and u_c is the manipulated variable. Note that when the valve characteristic and annulus density is known; it is also possible to utilize the valve equation (3.15).

The remaining parameters that needs to be identified are β_a, β_d, ρ_a, F_d, F_a, M_a and M_d. The following identification method for off-line estimation are suggested in the internal document [11].

Utilizing stationary measurements of choke pressure p_c and bottom-hole pressure p_a; the annulus and drill-string density and friction may be determined from the stationary equations for bit-flow and bit pressure

$$\begin{aligned} q_{bit} &= q_{pump} \\ p_p - p_c &= (F_d + F_a)q_{bit}^2 - (\rho_d - \rho_a)gh_{bit} \\ p_a - p_c &= F_a q_{bit}^2 + \rho_a g h_{bit} \end{aligned}$$

Here we have two equations with four unknowns. The number of equations may be expanded by measuring the pressures for different bit-flows q_{bit}, and solving for friction and density. A least square algorithm may be utilized to ensure a more accurate result.

A method for estimating fluid compressibility in the drill-string and annulus; β_d and β_a is suggested in [11]. The identification methods allow for estimation of parameters without the unknown bit-flow q_{bit}. In this report; off-line estimation of these parameter is not considered and the results from [11] is utilized in the simulations against Wemod and data from Grane. The parameters M_a and M_d are approximated by considering the average densities and applying equation (3.18).

4.2 Augmented model

For online estimation of a set of unknown time varying parameters; the model (3.20) is augmented as described in section 2.5. The augmented state vector is defined as

$$\mathbf{x} = \begin{pmatrix} p_p & p_c & q_{bit} & \theta \end{pmatrix}^T \tag{4.1}$$

where $\mathbf{x} \in \mathbb{R}^n$ and the vector θ contains the parameters to be estimated; here called parameter vector. The belonging state equations are

$$\mathbf{f}(\mathbf{x}) = \begin{pmatrix} \frac{\beta_d}{V_d}\left(q_{pump} - q_{bit}\right) \\ \frac{\beta_a}{V_a}\left(-\dot{V}_a + q_{bit} + q_{res} + q_{back} - q_{choke}\right) \\ \frac{1}{M_a + M_d}\left(p_p - p_c - F_d q_{bit}^2 - F_a(q_{bit} - q_{res})^2 + (\rho_d - \rho_a)gh_{bit}\right) \\ \mathbf{0} \end{pmatrix}$$

The augmented system can now be represented in the compact form

$$\dot{\mathbf{x}} = \mathbf{f}(\mathbf{x}) + \mathbf{w} \tag{4.2}$$

where $\mathbf{w}$ is a column vector of white noise processes with zero mean, covariance $E[ww^t] = Q$ and dimension $\mathbf{w} \in \mathbb{R}^n$

The measurement equation for the two measurements p_p and p_c is linear and given by

$$y_k = \begin{pmatrix} p_p \\ p_c \end{pmatrix} + \mathbf{v} \tag{4.3}$$

where the vector $\mathbf{v}$ is measurement noise and is normally distributed with covariance $E[vv^T] = R$. For the bottom-hole pressure; the measurement equation is given by

$$p_a = p_c + M_a\dot{q}_{bit} + F_a q_{bit}^2 + \rho_{a0} g h$$

In this report; estimation of q_{res} is not considered and so q_{res} is set to zero. Inserting $\dot{q}_{bit}$ and $q_{res} = 0$ into the above equation results in

$$\begin{aligned} p_a = {} & p_c + F_a q_{bit}^2 + \rho_{a0} g h_{bit} + \\ & \frac{M_a}{M_a + M_d}\left(p_p - p_c - F_d q_{bit}^2 - F_a q_{bit}^2 + (\rho_{d0} - \rho_{a0}) g h_{bit}\right) \end{aligned} \tag{4.4}$$

If we define M and $\bar{M}$ as

$$M \triangleq \frac{M_a}{M_a + M_d}, \quad \bar{M} = 1 - M = \frac{M_d}{M_a + M_d}$$

the measurement equation can be simplified to

$$\begin{aligned} p_a &= p_c\,(1 - M) + F_a q_{bit}^2\,(1 - M) + \rho_a g h_{bit}\,(1 - M) \\ &\quad + M(p_p - F_d q_{bit}^2 + \rho_d g h_{bit}) \\ &= \bar{M}(p_c + F_a q_{bit}^2 + \rho_a g h_{bit}) + M(p_p - F_d q_{bit}^2 + \rho_d g h_{bit}) \end{aligned}$$

Combining the measurement equation with measurements for p_p and p_c gives

$$\mathbf{h}(x) = \begin{pmatrix} p_p \\ p_c \\ \bar{M}(p_c + F_a q_{bit}^2 + \rho_a g h_{bit}) + M(p_p - F_d q_{bit}^2 + \rho_d g h_{bit}) \end{pmatrix} \tag{4.5}$$

The total system with state equations and measurement equations can now be described in the compact form

$$\begin{aligned} \dot{\mathbf{x}} &= \mathbf{f}(\mathbf{x}) + \mathbf{w} \\ \mathbf{y} &= \begin{cases} C\mathbf{x} \text{ ,with } p_p \text{ and } p_c \text{ measurement} \\ \mathbf{h}(\mathbf{x}) \text{ ,with } p_p,\ p_c \text{ and } p_a \text{ measurement} \end{cases} \end{aligned} \tag{4.6}$$

4.3 Observability

To obtain the correct parameter values when estimating the annulus parameters online; the augmented model needs to be observable. According to linear system theory (see for instance [9]) this can be determined by calculating the observability matrix; $\mathcal{O}$ and examine if the rank of $\mathcal{O}$ equals the dimension of the linearized state space model $\mathbf{f}(\mathbf{x}, \mathbf{u})$. The state space equations

$$\begin{aligned} \dot{x} &= Ax + Bu \\ y &= Cx \end{aligned}$$

for the augmented fluid model (4.6) is found by linearizing around the current operating point

$$A = \left.\frac{\partial f}{\partial x}\right|_{x=x^*,u=u^*} \quad B = \left.\frac{\partial f}{\partial u}\right|_{x=x^*,u=u^*} \quad C = \left.\frac{\partial h}{\partial x}\right|_{x=x^*} \tag{4.7}$$

where A is the state matrix, C is the measurement matrix, u is the control signal and B is the input matrix. The input matrix consists of mud-pump, back-pressure pump and choke valve, but it is not relevant for system observability. With a state matrix dimension of $A \in \mathbb{R}^n$; the observability matrix is given by

$$\mathcal{O} = \begin{pmatrix} C \\ CA \\ \vdots \\ CA^{n-1} \end{pmatrix}$$

An algebraic expression for the observability matrix is to intricate to display and to analyse. Instead; the observability matrix was calculated numerically by linearizing the model around some selected operating points. Observability was tested for both measurement equations; with and without p_a measurement. For the case with two measurements; p_p and p_c; the measurement equation is linear and given by

$$\mathbf{C} = \begin{pmatrix} 1 & 0 & 0 & \dots & 0 \\ 0 & 1 & 0 & \dots & 0 \end{pmatrix} \text{ ,where } \quad \mathbf{C} \in \mathbb{R}^{2\times n} \tag{4.8}$$

If p_a is available as a measurement or estimate the linearized measurement equation depends on the augmented state vector

$$C = \begin{pmatrix} 1 & 0 & 0 & 0 & \dots & 0 \\ 0 & 1 & 0 & 0 & \dots & 0 \\ M & \bar{M} & 2q_{bit}(F_a\bar{M} - F_dM) & \frac{\partial h_3}{\partial \theta_1} & \dots & \frac{\partial h_3}{\partial \theta_n} \end{pmatrix}_{x=x^*} \tag{4.9}$$

When the state vector is augmented with the parameter vector θ as

$$\begin{aligned} \theta &= \begin{pmatrix} \rho_a & F_a & \beta_a \end{pmatrix}, \text{ or} \\ \theta &= \begin{pmatrix} Cv & F_a & \beta_a \end{pmatrix} \end{aligned}$$

the observability matrix has $rank(\mathcal{O}) < dim(A)$ for both measurement equations; (4.8) and (4.9). This indicates that an EKF where all these parameters are estimated cannot be designed for this case. However; the model is observable when reducing the number of estimated parameters. For example; any augmented pairing of ρ_a, F_a, C_v and β_a is possible. An analysis for parameter convergence in the UKF has not been analyzed this report. Sufficient conditions for a bounded estimation error in the UKF can been found in [3].

4.4 Pragmatic approach to parameter estimation

In normal operation little excitation of the manipulated variables q_{pump}, q_{back} and z can be expected[11]. This implies that there will be long periods where the model and filter is stationary and the β parameters in equation (3.20) are cancelled. It is then possible estimate two stationary parameters[1]; or three if p_a is available. These estimated are independent of the value of β_a and β_d. Normally the observability problem would cause the Kalman filter to estimate a linear combination of the parameters and not the actual values, but due to the cancellation of β_a it should be possible to obtain the correct values.

When the system is stationary it is possible to identify the state q_{bit} and at most three more parameters. Equations (4.10) - (4.13) display the stationary case of the fluid model (3.20) and the bottom-hole measurement equation (3.21).

$$q_{pump} = q_{bit} \tag{4.10}$$

$$q_{choke} - q_{res} = q_{bit} + q_{back} \tag{4.11}$$

$$p_p - p_c = F_d q_{bit}^2 + F_a(q_{bit} + q_{res})^2 - (\rho_d - \rho_a) g h_{bit} \tag{4.12}$$

$$p_a - p_c = F_a(q_{bit} - q_{res})^2 + \rho_a g h_{bit} \tag{4.13}$$

From these equations we see that q_{bit} is given by the mud-pump. The unknown parameters in equation (4.11) are q_{res}, ρ_a and the valve constant C_v; if valve equation (3.15) is utilized. Annulus density and friction from equations (4.12) and (4.13) are associated with large uncertainty. These parameters enter in both equations, but it is still only possible to identify one of these in the stationary case. This is seen when writing out the bit-pressure p_a as seen from the drill-string

$$p_a = p_p + \rho_d g h_{bit} - F_d q_{bit}^2$$

Inserting for p_a in equation (4.13) gives equation (4.12); i.e, the two equations are linearly dependent, and we gain no new information useful for

[1] In this context; stationary parameters are the ones not cancelled when the given state equations are stationary

estimating F_a and ρ_a stationary. So, to be able to estimate F_a and ρ_a online we need excitation; which again requires the correct values for β_a and β_d.

The parameters β_d, β_a, M_d and M_a can only be estimated during transients.

4.4.1 Parameter estimation conclusions

Considering the points mentioned in this section; some estimation frameworks are suggested. As noted in the observability analysis; it is not feasible to estimate ρ_a, F_a and β_a at the same time in the Kalman filter. A possibility here is to determine ρ_a based on stationary off-line observations. For example; by measuring stationary pressures and flows and applying a least-squares algorithm to equations (4.10)-(4.13). The least-square result can be used to correct parameters not estimated online in the Kalman filter; such as annulus density ρ_a. Also; it should be tested whether it is possible to estimate ρ_a and F_a during excitation; and how this estimation is affected by error in the fluid bulk-modulus.

Since annulus density and the choke valve characteristic is not know; there are uncertainties associated with the choke-flow q_{choke}. If a measurement of this flow is not available; C_v can be estimated together with the annulus friction and bulk-modulus. The parameter vector for the stationary filter can then be represented as

$$\theta_{\mathbf{s}} = \begin{pmatrix} C_v & F_a \end{pmatrix}$$

whereas the transient parameter vector is

$$\theta_{\mathbf{d}} = \begin{pmatrix} \beta_a \end{pmatrix}$$

When the bit-flow is zero; it is not possible to estimate either friction or fluid bulk-modulus. In this situation the parameter vector is empty and only the bit-flow is estimated. Also, since there might arise problems as $q_{bit} \to 0$; the parameter estimation should be turned off in advance.

The parameter vectors suggested require that transients and stationary conditions are know. Since excitations from the choke-valve and mud-pump is known beforehand; it should be possible to shift between the stationary and transient Kalman filters and obtain a correct estimate. To ensure a correct estimate when switching between filters; the stationary parameters must converge before changing filter.

4.5 Discretization of augmented model

For implementation purposes; the augmented state equations are converted to difference equations. This was accomplished by applying Euler's method

for numerical integration on equation (4.2). The discrete model is given by

$$\begin{aligned}
f_1 &= p_{p_{k+1}} = p_{p_k} + h\frac{\beta_d}{V_d}\left(q_{pump_k} - q_{bit_k}\right) + hw_{k_1} \\
f_2 &= p_{c_{k+1}} = p_{c_k} + h\frac{\beta_a}{V_a}\left(-\dot{V}_a + q_{bit_k} + q_{res_k} + q_{back_k} - zA_cK_c\sqrt{\frac{2}{\rho_{a0}}(p_{c_k} - p_0)}\right) + hw_{k_2} \\
f_3 &= q_{bit_{k+1}} = q_{bit_k} + \frac{h}{M_a + M_d}\left(p_p - p_c - F_d q_{bit}^2 - F_a(q_{bit} - q_{res})^2 + (\rho_{d0} - \rho_{a0})gh_{bit}\right) + hw_{k_3} \\
f_{\theta_1} &= \theta_{1,k+1} = \theta_{1,k} \\
&\vdots \\
f_{\theta_n} &= \theta_{n,k+1} = \theta_{n,k}
\end{aligned} \tag{4.14}$$

where h is the discrete time shift. According to [4]; Euler's method for numerical integration is stable for

$$h \leq -\frac{2}{\lambda} \tag{4.15}$$

where λ is the smallest eigenvalue of the continuous state equations. The choke pressure equation from the process model (3.20) is given by

$$\frac{V_a}{\beta_a}\dot{p}_c = -\dot{V}_a + q_{bit} + q_{res} + q_{back} - zA_cK_c\sqrt{\frac{2}{\rho_{a0}}\Delta p_c} \tag{4.16}$$

When all inputs are zero the linearized pressure equation can be written as

$$\dot{p}_c = -\frac{C}{2\sqrt{\Delta p_c}}, \text{ where } \quad C = \frac{\beta_a}{V_a}zA_cK_c\sqrt{\frac{2}{\rho_a}} \tag{4.17}$$

The eigenvalues for the linearized system is

$$\lambda = -\frac{C}{\sqrt{\Delta p_c}} \tag{4.18}$$

As we can see from the equation above; the eigenvalue $\lambda \to -\infty$ as $\Delta p_c \to 0$. According to the stability requirement (4.15); the discrete system is locally unstable. This will cause oscillations around $q_{bit} = 0$, and might lead to problems in the Kalman filters. Especially in the UKF, where a negative definite covariance matrix causes imaginary values when calculating the matrix square root. One solution is utilizing another valve equation. In [4, chapter 4] a valve equation with smooth transition between laminar flow; $q = C_l\Delta p$; and turbulent flow is suggested. The problem may also be solved by increasing the bit-flow process noise covariance during low bit-flows. Another way of solving the problem is to utilize an implicit integration solver that is stable for the hole left half plane.

Chapter 5

Kalman filter design

This chapter presents an overview of the implemented EKF and UKF. Based on the conclusions from the former chapter; the Kalman filter must be able to switch between estimated parameters. In the EKF this involve designing a different filter for each set of parameters and changing between filters. For the UKF this can be accomplished by utilizing the same filter. It is assumed that the process noise and measurement noise is diagonal and not correlated with each other.

5.1 Extended Kalman filter design

Parameter vectors considered in the EKF are

$$\theta = \begin{pmatrix} \rho_a & F_a & \beta_a \end{pmatrix} \tag{5.1}$$

$$\theta = \begin{pmatrix} F_a & \beta \end{pmatrix} \tag{5.2}$$

$$\theta_{\mathbf{s}} = \begin{pmatrix} F_a \end{pmatrix} \quad \theta_{\mathbf{d}} = \begin{pmatrix} \beta_a \end{pmatrix} \tag{5.3}$$

The observability analysis indicated an observability problem when estimating annulus density, friction and bulk-modulus at the same time. The first parameter vector in the list above is included only to verify this and to compare it to the UKF.

As mentioned in section 2.3; the EKF approximates the propagated mean as

$$E\left[\mathbf{f}(\mathbf{x})\right] \approx \mathbf{f}(\bar{\mathbf{x}})$$

The apriori error covariance matrix is approximated by considering a linearization around the current estimate, and calculating the propagation through the linear system. To design the filter we must therefore augment the state equations and determine the state matrix $\mathbf{A}$.

5.1.1 EKF with parameter vector $\theta = (\rho_a \quad F_a \quad \beta_a)$

As an example the augmentation of the first parameter vector in (5.1) is shown. The state equations are

$$\begin{aligned}
p_{p_{k+1}} &= p_{p_k} + h\frac{\beta_d}{V_d}\left(q_{pump_k} - q_{bit_k}\right) + hw_1 \\
p_{c_{k+1}} &= p_{c_k} + h\frac{\beta_a}{V_a}\left(-\dot{V}_a + q_{bit_k} + q_{res_k} + q_{back_k} - q_{choke}\right) \\
q_{bit_{k+1}} &= q_{bit_k} + \frac{h}{M_a + M_d}\left(p_p - p_c - F_d q_{bit}^2 - F_a(q_{bit} - q_{res})^2 + (\rho_{d0} - \rho_{a0})g h_{bit}\right) + hw_3 \\
\rho_{a,k+1} &= \rho_{a,k} + hw_4 \\
F_{a,k+1} &= F_{a,k} + hw_5 \\
\beta_{a,k+1} &= \beta_{a,k} + hw_6
\end{aligned} \tag{5.4}$$

and the belonging Jacobian matrix with state vector $\mathbf{x} = \begin{pmatrix} p_P & p_c & q_{bit} & \rho_a & F_a & \beta_a \end{pmatrix}$ is

$$\mathbf{A}_k = \frac{\partial \mathbf{f}}{\partial \mathbf{x}} = \begin{pmatrix}
1 & 0 & -\frac{\beta_d}{V_d} & 0 & 0 & 0 \\
0 & \frac{\partial f_2}{\partial p_c} & \frac{\beta_a}{V_a} & \frac{\partial f_2}{\partial \rho_a} & 0 & \frac{\partial f_2}{\partial \beta_a} \\
\frac{1}{M_a+M_d} & \frac{-1}{M_a+M_d} & \frac{\partial f_3}{\partial q_{bit}} & \frac{-g h_{bit}}{M_a+M_d} & \frac{-(q_{bit}-q_{res})^2}{M_a+M_d} & 0 \\
0 & 0 & 0 & 1 & 0 & 0 \\
0 & 0 & 0 & 0 & 1 & 0 \\
0 & 0 & 0 & 0 & 0 & 1
\end{pmatrix} \tag{5.5}$$

where the unspecified terms; $\partial f/\partial x$ are shown in appendix B. The measurement equation for filtrating the estimated state and covariance depends on the measurements available. When p_p and p_c are measured the measurement equation is given by (4.8), and when p_a is included; the linearized measurement equation (4.9) is utilized. Initial conditions for the state vector are

$$x_a = \begin{pmatrix} p_{p,0} & p_{c,0} & q_{bit,0} & \rho_{a,0} & F_{a,0} & \beta_{a,0} \end{pmatrix}^T \tag{5.6}$$

with the corresponding initial error covariance matrix

$$P_{k,0} = \begin{pmatrix}
\Delta p_{p,0}^2 & 0 & 0 & 0 & 0 & 0 \\
0 & \Delta p_{c,0}^2 & 0 & 0 & 0 & 0 \\
0 & 0 & \Delta q_{bit,0}^2 & 0 & 0 & 0 \\
0 & 0 & 0 & \Delta \rho_{a,0}^2 & 0 & 0 \\
0 & 0 & 0 & 0 & \Delta F_{a,0}^2 & 0 \\
0 & 0 & 0 & 0 & 0 & \Delta \beta_{a,0}^2
\end{pmatrix} \tag{5.7}$$

The initial error covariance matrix is a measure of the uncertainty in the initial values of the state vector (5.6). The EKF with parameter vectors

(5.2) and (5.3) is simply obtained from (4.14) and computing the belonging Jacobin according to (2.11). An overview of the EKF algorithm is displayed in appendix A.1.

5.1.2 Changing between estimated parameters

To be able to swith between estimated parameters online in the EKF; one filter was designed for each parameter vector. The filters designed where; one for stationary conditions, one for transients and one when q_{pump} is under a certain value. The transient mode was set based on pump or valve movement of a given size; plus a time period to let the system obtain its stationary state. For the filters to maintain its previous state after a swith, the value of the belonging state and covariance where saved in each iteration. The saved states and parameters where set to constants when utilized in another filter.

5.2 Unscented Kalman filter design

As mentioned in section 2.4; the UKF utilizes the unscented transform for calculating the mean and covariance propagated through the state and measurement equations. Process and measurement noise is incorporated in the propagation of sigma-points by expanding the state vector and error covariance matrix as

$$x_a = \begin{pmatrix} x_n \\ v_k \\ w_k \end{pmatrix} \qquad P_{a_{xx}} = \begin{pmatrix} P_{xx} & 0 & 0 \\ 0 & Q & 0 \\ 0 & 0 & R \end{pmatrix}$$

where

$$E[w_k w_k^T] = 0 \qquad E[v_k v_k] = 0$$

The new state vector has dimension $x_a \in \mathbb{R}^{2n+m}$, where n is the dimension of the augmented state vector and m is the number of measurements. This means that the number of calculated sigma-points are $2(2n+m)+1$. The sigma-points are placed in the matrix

$$\mathcal{X}_{k-1}^a = \begin{pmatrix} \hat{\mathbf{x}}_{\mathbf{k-1}}^{\mathbf{a}} & \hat{\mathbf{x}}_{\mathbf{k-1}}^{\mathbf{a}} + \sqrt{(N+\lambda)\mathbf{P}_{\mathbf{k-1}}^{\mathbf{a}}} & \hat{\mathbf{x}}_{\mathbf{k-1}}^{\mathbf{a}} - \sqrt{(N+\lambda)\mathbf{P}_{\mathbf{k-1}}^{\mathbf{a}}} \end{pmatrix}$$

with dimension $\mathcal{X}_{k-1}^a \in \mathbf{R}^{(2n+m)\times(2(2n+m)+1)}$. The first $2n$ rows of the matrix $\mathcal{X}_{k-1}^x$ and $\mathcal{X}_{k-1}^w$; associated with the error covariance P_k and process noise Q are propagated through the state equations

$$\mathcal{X}_{k|k-1}^x = \mathbf{f}(\mathcal{X}_{k-1}^x, \mathcal{X}_{k-1}^w),$$

whereas the first n rows $\mathcal{X}_{k-1}^x$ and last m rows $\mathcal{X}_{k-1}^v$ are propagated through the measurement equation

$$\mathcal{Y}_{k|k-1} = \mathbf{h}(\mathcal{X}_{k-1}^x, \mathcal{X}_{k-1}^v) \tag{5.8}$$

If the measurement equation is linear; as in the situation when measuring p_p and p_c; the measurement update may be computed according to the classical Kalman filter equations

$$\begin{aligned} \hat{y}_k &= C\hat{x}_k^- \\ P_{yy} &= CP_k^-C^T + R \\ P_{xy} &= P_k^-C^T \\ \hat{x}_k &= \hat{x}_k^- + P_{xy}P_{yy}^{-1}(y_k - \hat{y}_k) \\ P_k &= P_k^- - P_{xy}P_{yy}^{-1}P_{xy}^T \end{aligned} \tag{5.9}$$

and the measurement propagation in equation (5.8) is omitted.

5.2.1 UKF with parameter vector $\theta = (\rho_a \;\; F_a \;\; \beta_a)$

Here the same example shown for the EKF is presented. The state equations are given by the augmented model (5.4). The initial state vector is

$$x_a = \begin{pmatrix} x_{k,0} & 0 & 0 & 0 & 0 & 0 & 0 & 0 & 0 \end{pmatrix}^T$$

with the corresponding initial error covariance matrix

$$P_{a,0} = \begin{pmatrix} P_{k,0} & 0 & 0 \\ 0 & Q & 0 \\ 0 & 0 & R \end{pmatrix}$$

where $x_{k,0}$ and $P_{k,0}$ is given by (5.6) and (5.7). From these initial conditions the UKF algorithm in appendix A.2 is applied.

5.2.2 Changing estimated parameters

Changing between estimated parameter-sets in the UKF can be performed simply by freezing and unfreezing the corresponding sigma-points before they are propagated through the process model. To explain this further; an example where estimation of one parameter in a nonlinear function is turned on and off. Let the augmented process model be

$$\begin{aligned} x_{k+1} &= x_k + f(x_k, \theta_k) + hw_1 \\ \theta_{k+1} &= \theta_k + hw_2 \end{aligned} \tag{5.10}$$

with an error covariance matrix and process noise covariance matrix

$$P_k = \begin{pmatrix} p_{11} & p_{12} \\ p_{21} & p_{22} \end{pmatrix} \qquad Q = \begin{pmatrix} q_{11} & 0 \\ 0 & q_{22} \end{pmatrix}$$

The augmented state vector and covariance matrix are

$$x_k^a = \begin{pmatrix} x_k & \theta_k & 0 & 0 \end{pmatrix}^T \qquad P_k^a = \begin{pmatrix} P_k & 0 \\ 0 & Q \end{pmatrix} \tag{5.11}$$

Calculating the matrix square root and the sigma-points results in the matrices

$$S = \sqrt{(\lambda + n)P_k^a} = \begin{pmatrix} s_{11} & s_{12} & 0 & 0 \\ s_{21} & s_{22} & 0 & 0 \\ 0 & 0 & s_{33} & 0 \\ 0 & 0 & 0 & s_{44} \end{pmatrix}$$

$$\mathcal{X}_{k-1}^a = \begin{pmatrix} \hat{x}_{k-1}^a & \hat{x}_{k-1}^a \pm S_i \end{pmatrix}$$
$$= \begin{pmatrix} x_k & x_k + s_{11} & x_k + s_{12} & x_k & x_k & x_k - s_{11} & x_k - s_{12} & x_k & x_k \\ \theta_k & \theta_k + s_{21} & \theta_k + s_{22} & \theta_k & \theta_k & \theta_k - s_{21} & \theta_k - s_{22} & \theta_k & \theta_k \\ 0 & 0 & 0 & q_{11} & 0 & 0 & 0 & -q_{11} & 0 \\ 0 & 0 & 0 & 0 & q_{22} & 0 & 0 & 0 & -q_{22} \end{pmatrix}$$

Each column vector in the matrix above represents one sigma-point for the augmented state vector x_k^a, and one by one the column vectors are propagated through the augmented process model (5.10). Halting the θ parameter is now achieved by assigning all entries in the second row equal to the first element in the row, and all elements in the last row to zero

$$\mathcal{X}_{k-1}^a = \begin{pmatrix} x_k & x_k + s_{11} & x_k + s_{12} & x_k & x_k & x_k - s_{11} & x_k - s_{12} & x_k & x_k \\ \theta_k & \theta_k & \theta_k & \theta_k & \theta_k & \theta_k & \theta_k & \theta_k & \theta_k \\ 0 & 0 & 0 & q_{11} & 0 & 0 & 0 & -q_{11} & 0 \\ 0 & 0 & 0 & 0 & 0 & 0 & 0 & 0 & 0 \end{pmatrix}$$

This will allow the θ parameter to be unchanged after propagation. The sum of the weights utilized for determining the final value of θ_k equals one, and thus; the parameter remains equal to the last time step. To be able to unfreeze the parameter; the belonging error covariance elements of P_k must be saved before estimation of the parameter is halted. When estimation is resumed; the error covariance elements corresponding to the parameter are restored.

5.3 Constraint handling in the EKF and UKF

Another important part of state and parameter estimation is constraint handling. Figure 5.1 display a schematic in two dimensions of how constraints can be performed in the EKF and UKF. In the EKF; this is simply performed by moving the predicted states and parameters to the violated constraint. For the states; this involve keeping the absolute pressure and bit-flow non-negative. As seen from the figure; the error covariance is not affected by moving the state or parameters. In the UKF; constraint handling is per-

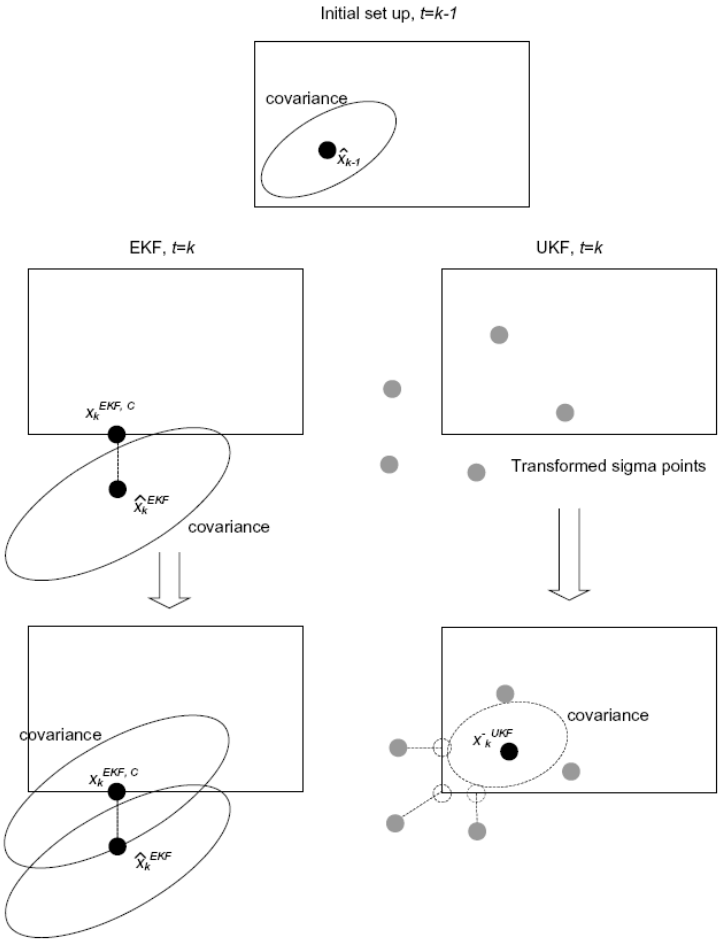

Figure 5.1: Constraint handling in the EKF and UKF

formed be moving all propagated sigma-points back to the violated constraint. This ensures that the computed mean is within the constraints. The error covariance matrix is also affected by the constraint handling, and thus contains information about the nearby constraint as the computed covariance is smaller [1].

5.4 Covariance tuning

Several methods for online tuning of the covariance matrices Q and R where attempted, see for instance [14], [15], [8] or [2]. All these methods rely on a linear observable state space model. The idea was to implement a linearized model during stationary conditions and apply the method proposed in [14] to the original process model. The method was implemented for the linearized versions of the state equations (3.20).

Since the model is also utilized for parameter estimation; online tuning of the covariance matrices might not be the best solution. Instead the covariances where determined by calculating an initial value according to Bryson's inverse quadratic method. The covariances where then tuned to obtain a satisfactory result.

Assuming the process noise and measurement noise covariance matrices is not correlated mutually or between each other

$$Q_0 = diag(q_1, q_2, \dots q_n) \quad R = diag(r_1, r_2 \dots r_m)$$

an initial value for the process noise and measurement noise covariances can be determined with Bryson's inverse quadratic method.

1. Assign the maximum allowed estimation deviation as $\delta x_i = max(|x_i - \hat{x}_i|)$ and calculate
$$\left\{ q_i = \frac{1}{(\delta x_i)^2} \right\}^n$$
2. Choose the measurement matrix elements as
$$\left\{ r_j = \frac{1}{(\delta y_j)^2} \right\}^n$$

where $\delta y_j = |y_i - \bar{y}_j|$, and $\bar{y}_j$ is the mean of stationary measurement, and y_j is the maximum observed measurement deviation from this mean. When the elements in the covariance matrices have been determined; the filter is tuned according to

$$Q_k = \sigma Q_0$$

where σ is a scalar value that determines the scaling between R_k and Q_k.

To get an acceptable estimation of the bottom-hole pressure; it is important to not add to much uncertainty in the process model. The uncertainty was therefore added to the estimated parameters. For example; if to much uncertainty is combined with q_{bit}; it is impossible to obtain a correct friction estimate.

Chapter 6

Observer performance and robustness

To verify that the estimated states and parameters converge to the correct values; the EKF and UKF algorithms where tested against data obtained from simulations on the design model (3.20). To be able to compare the UKF and EKF; the same noise set was utilized in simulations of both filters. The covariance matrices where also equal in the EKF and UKF. All parameters in the design model and Kalman filters are identical; except for the ones estimated. The parameters utilized in the simulations are displayed in table 6.1.

Parameter	Value	Description
p_0	1 bar	Atmospheric pressure
$\bar{\rho}_a$	$1250\,\mathrm{kg/m^3} \cdot 10^{-5}$	Average annulus density
$\bar{\rho}_a$	$1250\,\mathrm{kg/m^3} \cdot 10^{-5}$	Average drill-string density
F_a	20800	Annulus friction factor
F_d	165000	Drill-string friction factor
M_a	5730	Annulus mass coefficient
M_d	5730	Drill-string mass coefficient
β_a	14000	Annulus bulk-modulus
β_a	14000	Drill-string bulk-modulus
V_a	$28.27\,\mathrm{m^3}$	Annulus volume
V_d	$96.13\,\mathrm{m^3}$	Drill-string volume
h_{bit}	2000 m	Well depth
l_{bit}	3600 m	Well length
L_{dN}	3600 m	Drill-string length
K_c	0.0046	Choke valve constant
A_c	$0.04\,m^2$	Choke valve opening

Table 6.1: Design model parameters

6.1 Input excitation and parameter estimation

First the Kalman filters where simulated with excitations from the mud-pump to determine how accurate they can estimate the unknown parameters. The back-pressure pump and choke valve where maintained constant during the simulation.

6.1.1 Estimation of ρ_a, F_a and β_a

Ideally the parameters ρ_a, F_a and β_a should be estimated at the same time. According to the observability analysis in section 4.3 this is not possible. To verify this the UKF and EKF where augmented with the parameter vector

$$\theta = \begin{pmatrix} \rho_a & F_a & \beta_a \end{pmatrix}$$

All parameter and the state; q_{bit} where here estimated at the same time. The initial values for the parameters where set to

Parameter	Value
$q_{bit,0}$	1000 l/min
$p_{p,0}$	74 bar
$p_{c,0}$	125 bar
$\rho_{a,0}$	1150 kg/m^3
$F_{a,0}$	15800
$\beta_{a,0}$	9000

Table 6.2: Initial state and parameter values

The measured and estimated parameters; along with mud-pump excitations are displayed in figure 6.1. Figure 6.2 and 6.3 present the deviation from the desired states and parameters. The left column of the figures show the initial estimation transient, and the right column display the response for the remaining simulation period. It is not possible to see the error between the measured states p_p and p_c and the states filtrated by the UKF since the scaling is to large. Figure As can be seen from figures 6.1 and 6.2; both the EKF and UKF computes an accurate estimate of the bottom-hole pressure and bit-flow, even though the augmented model is not observable. However; in the parameter deviation plot 6.3; we see that the EKF does not converge to the correct parameter values. The UKF approximates the nonlinearities better and the parameter error converges to zero.

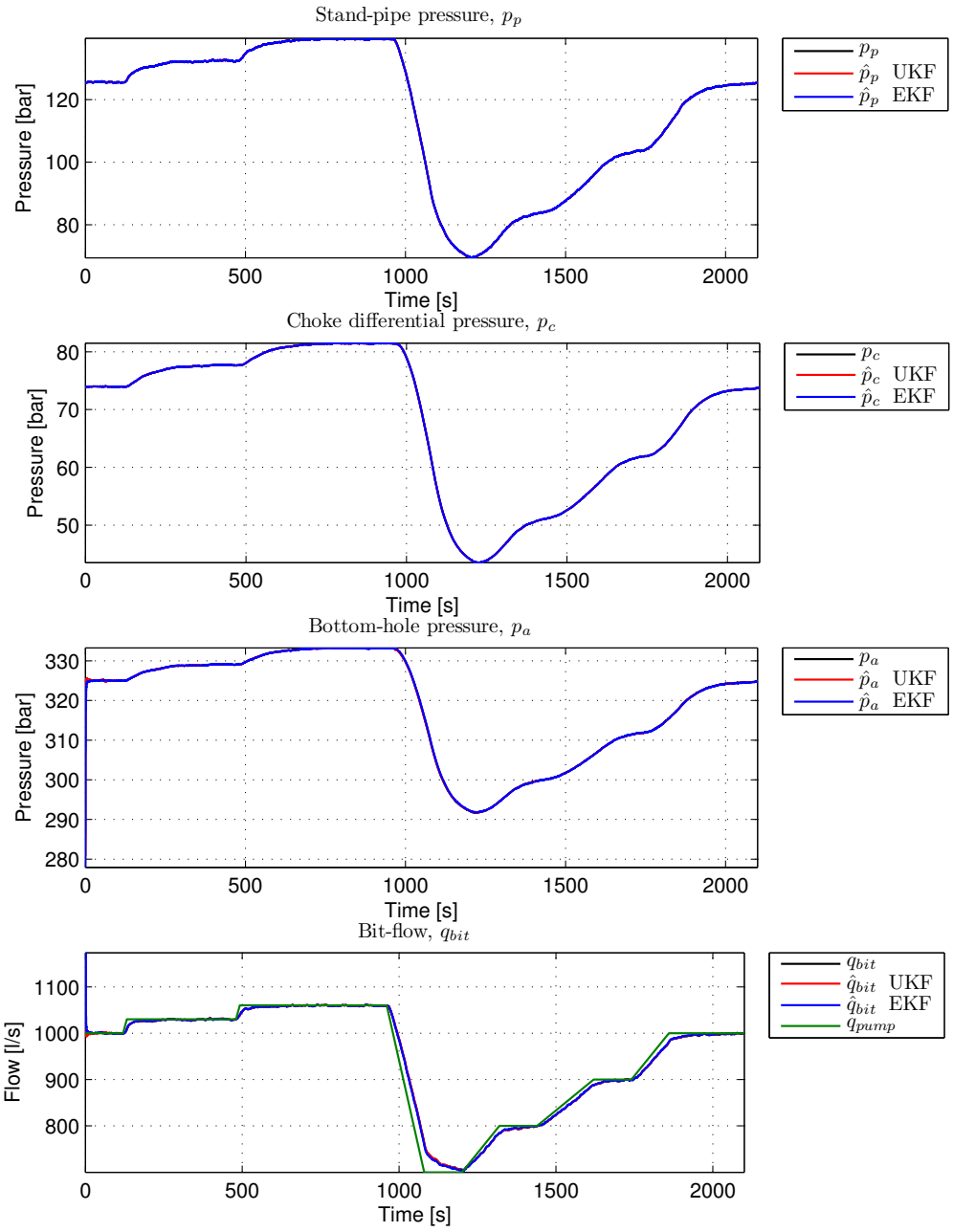

Figure 6.1: Pressure estimation when estimating ρ_a, F_a and β_a with UKF and EKF

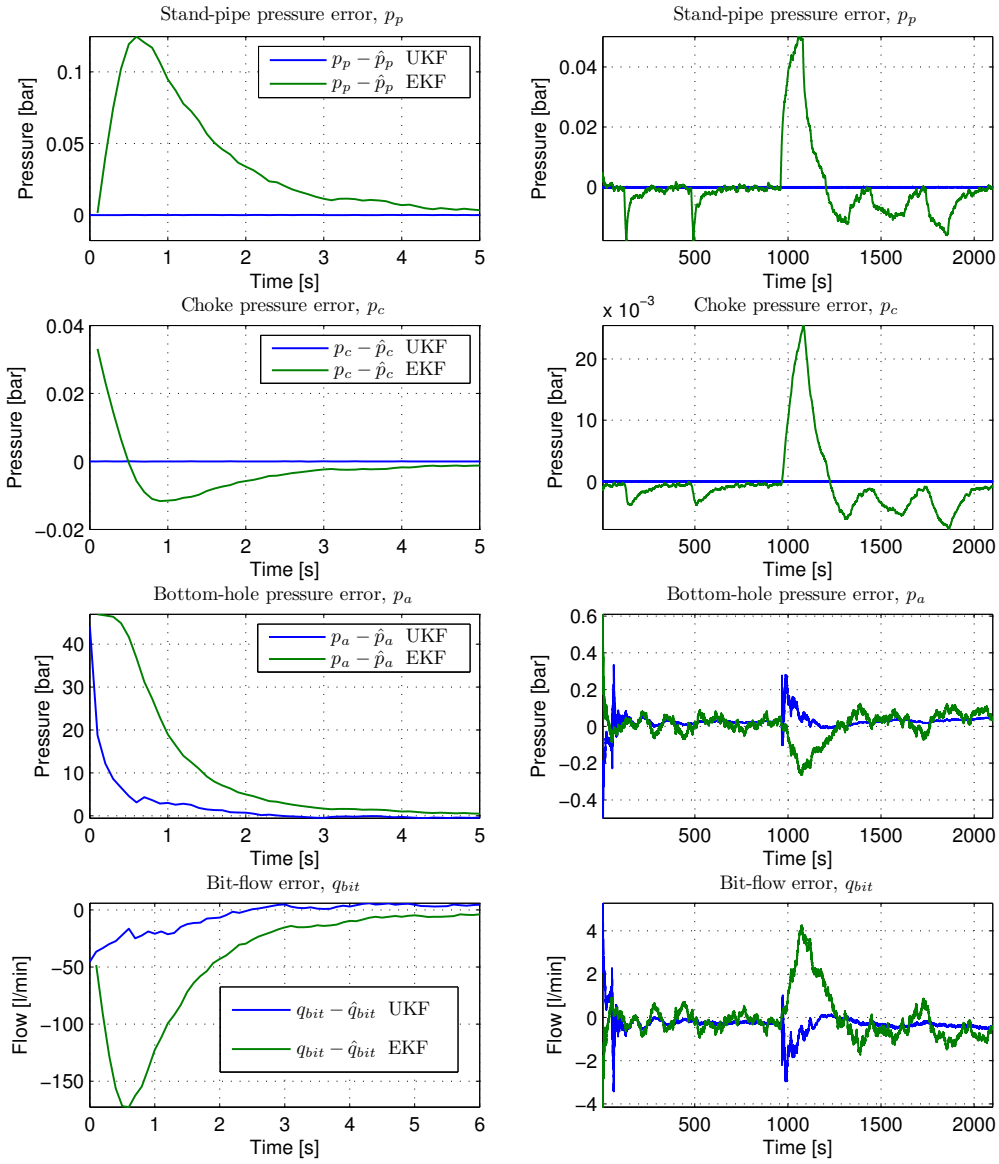

Figure 6.2: Pressures estimation error when estimating ρ_a, F_a and β_a with UKF and EKF

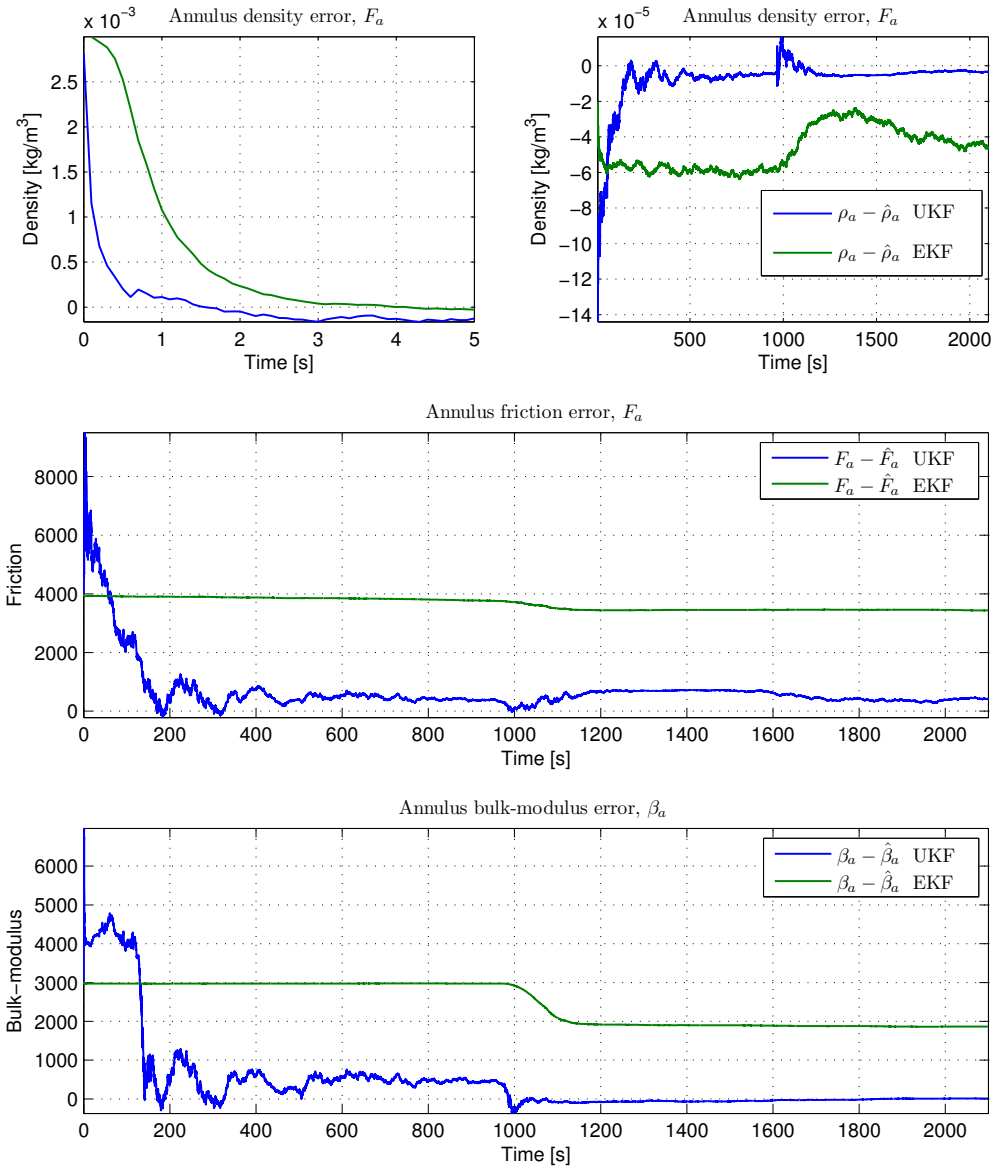

Figure 6.3: Parameter estimation error when estimating ρ_a, F_a and β_a with UKF and EKF

6.1.2 Estimation of F_a and β_a

When augmenting the process model with F_a and β_a the system is observable and it should be possible to estimate correct values for these parameters. Initial values for q_{bit}, F_a and β_a where set as in table 6.2. In this simulation annulus friction was estimated during stationary conditions, and fluid bulk modulus was estimated during transients. Simulation scenarios where both parameters where estimated at the same time has also been conducted, but this did not give as good results.

In this simulation; the data from the design model where obtained with Euler's method; described in section 2.1. Since the method has a fixed step size; the process noise added to p_p and p_c is known, and the Kalman filter covariance matrices could be determined directly.

To measure the difference between the EKF and UKF the Integral Square Error (ISE) was computed on the bottom-hole pressure difference according to

$$ISE = \sum_{i=0}^{n} |p_a - \hat{p}_a|^2 \Delta t$$

The results of the ISE where

$$ISE_{UKF} = 2.4 \quad ISE_{EKF} = 18.4$$

This shows that the UKF performs better than the EKF; with an ISE of over 7 times larger in the EKF. Figure 6.4 display the pressure progress; and both filters estimate a correct bit-flow and bottom-hole pressure. The errors from the real values are displayed in figure 6.2, and we see that the UKF converges a little bit faster than the EKF. In figure 6.1.2 we also see that the parameters converge converges faster in the UKF and that the final values in the UKF lie closer to the correct value.

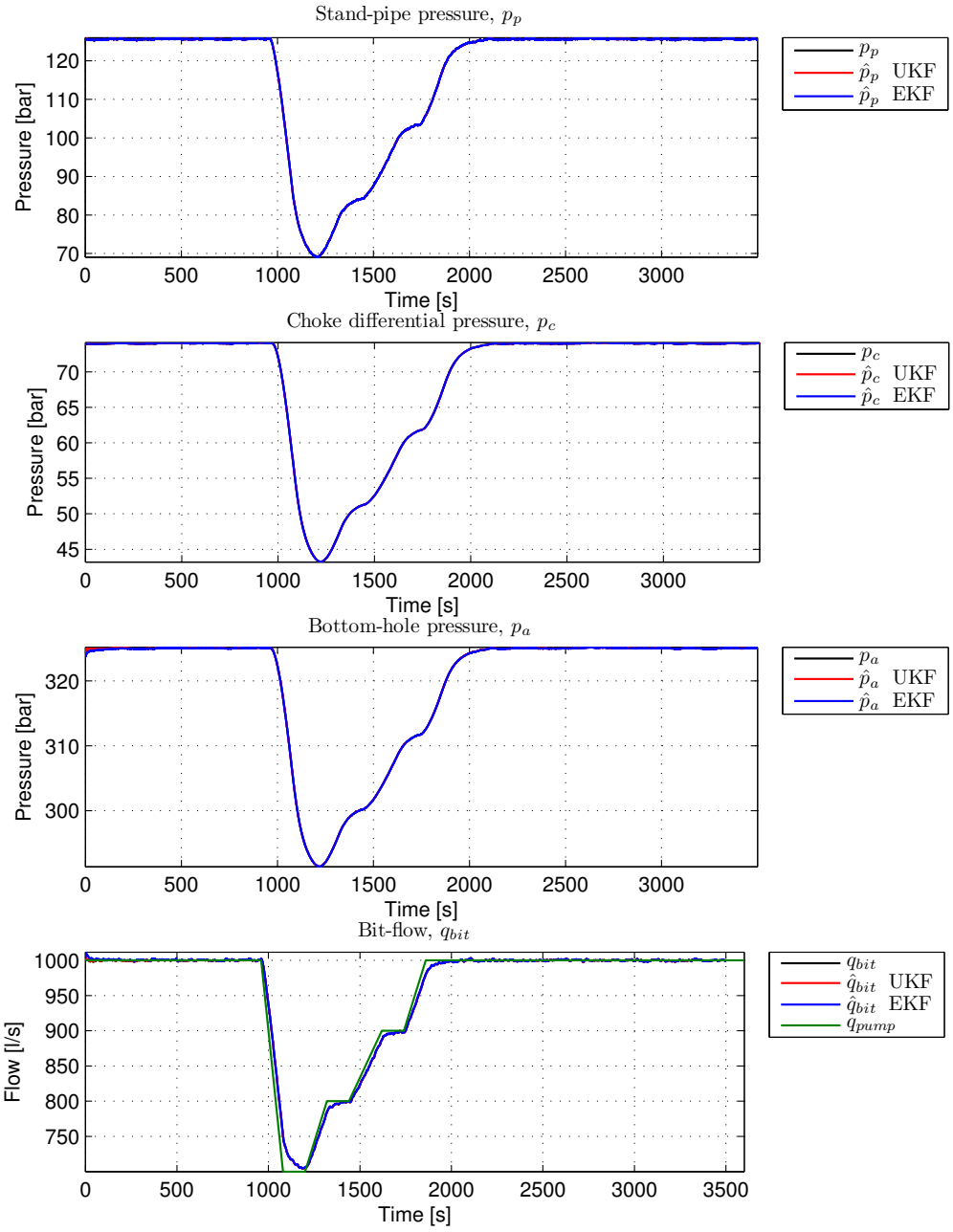

Figure 6.4: Pressure when estimating F_a and β_a with UKF and EKF

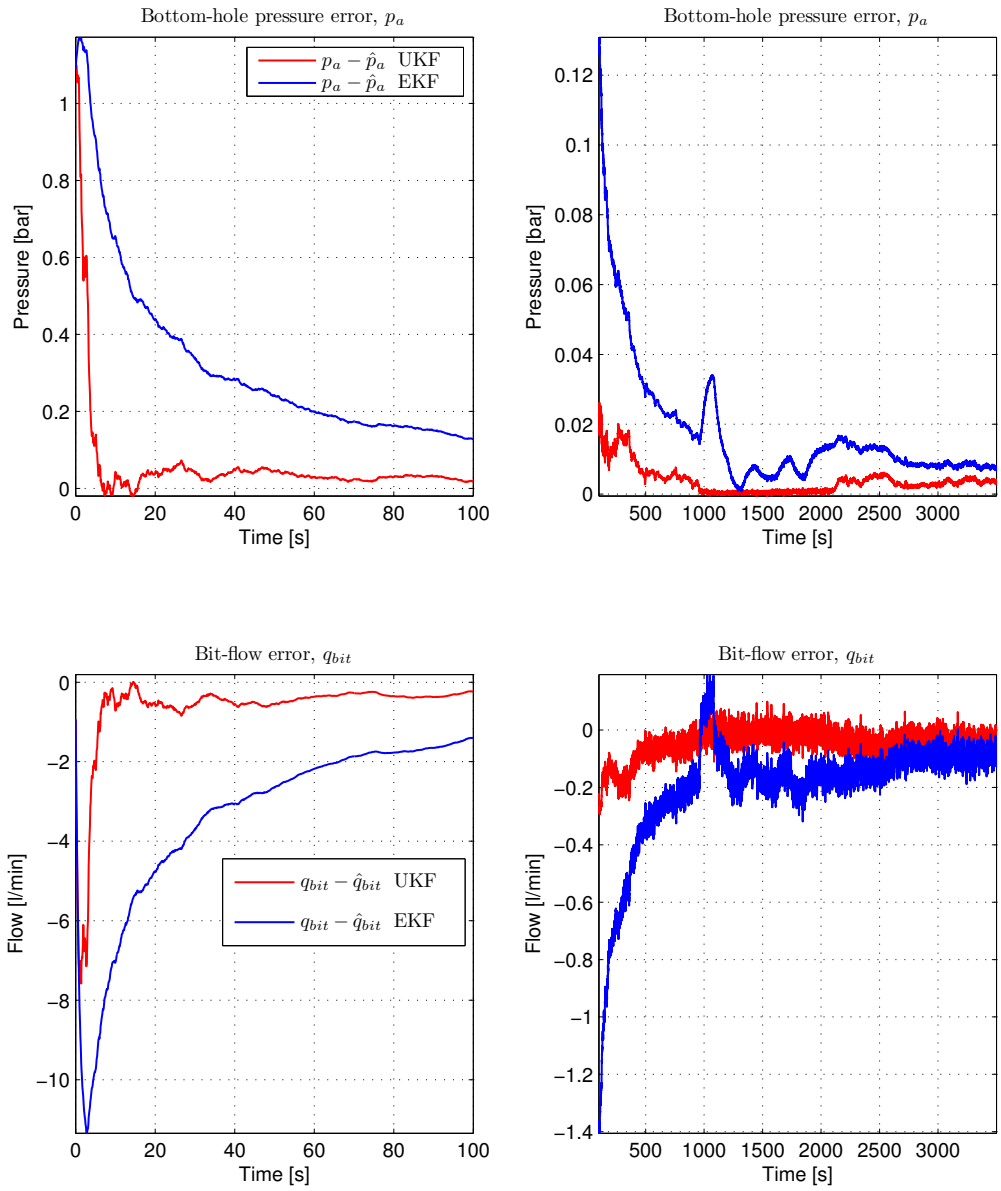

Figure 6.5: Pressure error when estimating F_a and β_a with UKF and EKF

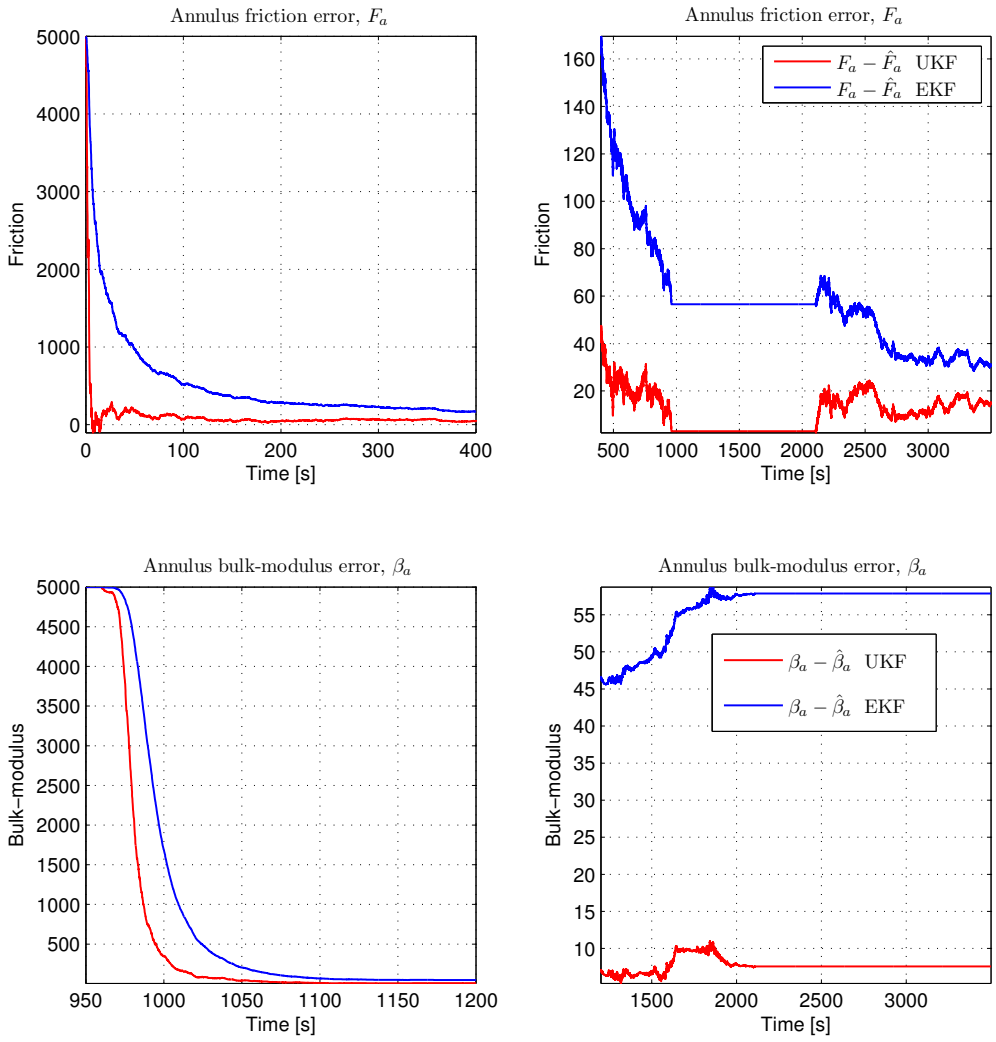

Figure 6.6: Parameter estimation when estimating F_a and β_a with UKF and EKF

6.2 Pipe-connection and filter switching

In the pipe-connection scenario; F_a was estimated during stationary conditions and β_a was estimated during transients. Since there are some problems with numerically stability when $q_{bit} \rightarrow 0$; the data from the design model had to be computed by a solver with variable step size. The added process noise was therefore not known and the covariance matrices had to be tuned.

Figures 6.7 - 6.9 display the estimated states and parameters during a pipe-connection. The initial values where set as in table 6.2; When the mud-pump is ramped down from $q_{pump} = 1000$ l/min to 0; the back-pressure pump was ramped up from 200 l/min to 400 l/min. At the same time the friction estimation is turned off and the filters starts to estimate β_a. When the bit-flow approach 100 L/s; the parameter estimation is turned off and only q_{bit} is estimated. Figure 6.7 display both estimated and real pressures. It is not possible to see any difference between estimated and real pressures; the plots are merely shown to see the pressure and bit-flow progress. Instead the state errors can be seen in figure 6.8. Both filters estimates the correct values, but the UKF converges faster. The ISE values for the UKF and EKF are

$$ISE_{UKF} = 645 \quad ISE_{EKF} = 893$$

The large ISE-values are the result of larger process noise variances than in the previous scenario, and that the filters deviates somewhat from the true bottom-hole pressure when $q_{bit} = 0$. As seen from the parameter estimation 6.9; it is theoretically possible to exploit the dynamics during pump-shut down to estimate β_a. The figure also show that the UKF converges faster and closer to the correct value than the EKF.

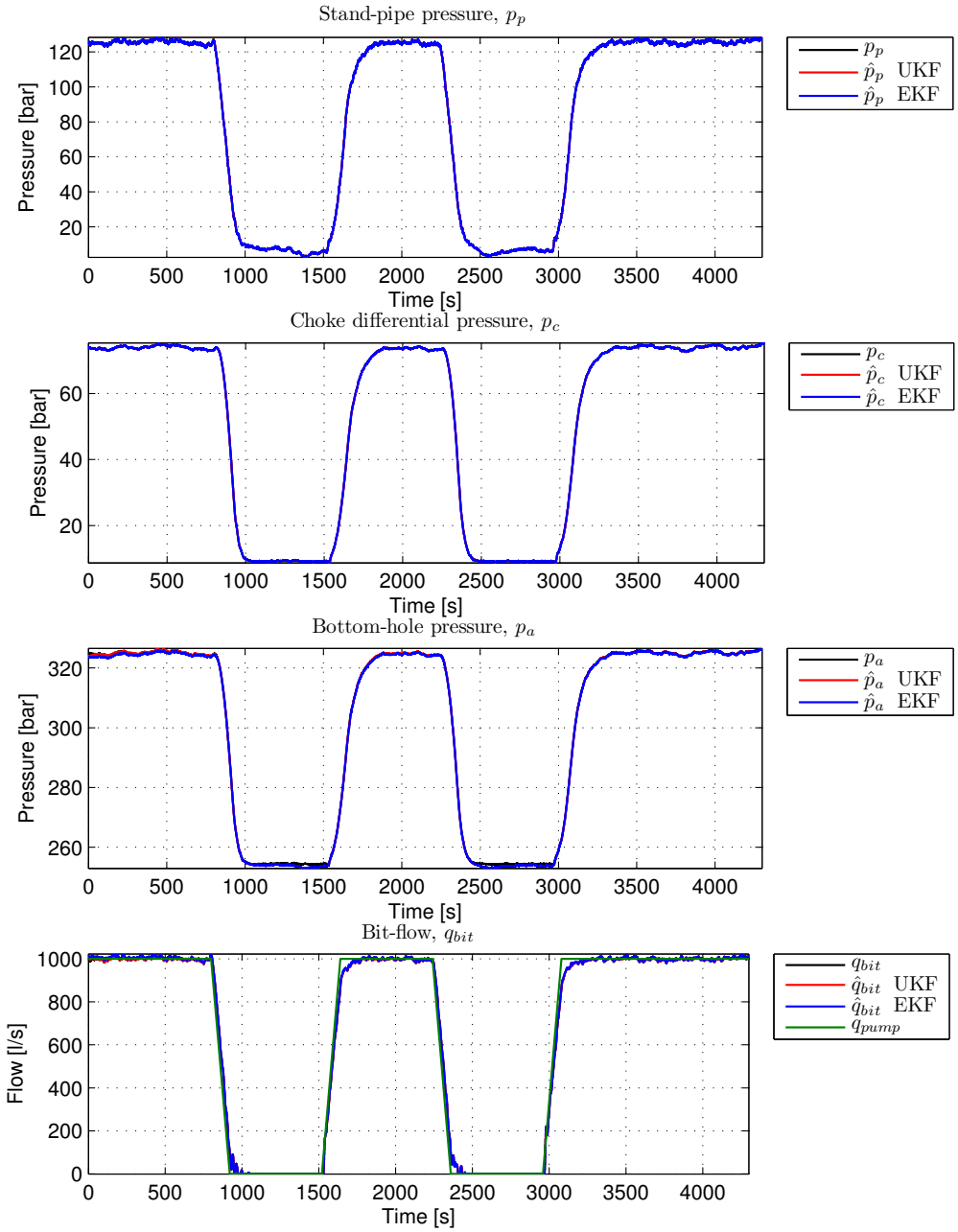

Figure 6.7: Pressure estimation during pipe-connection. Switching between F_a and β_a

The deviation in figure 6.8

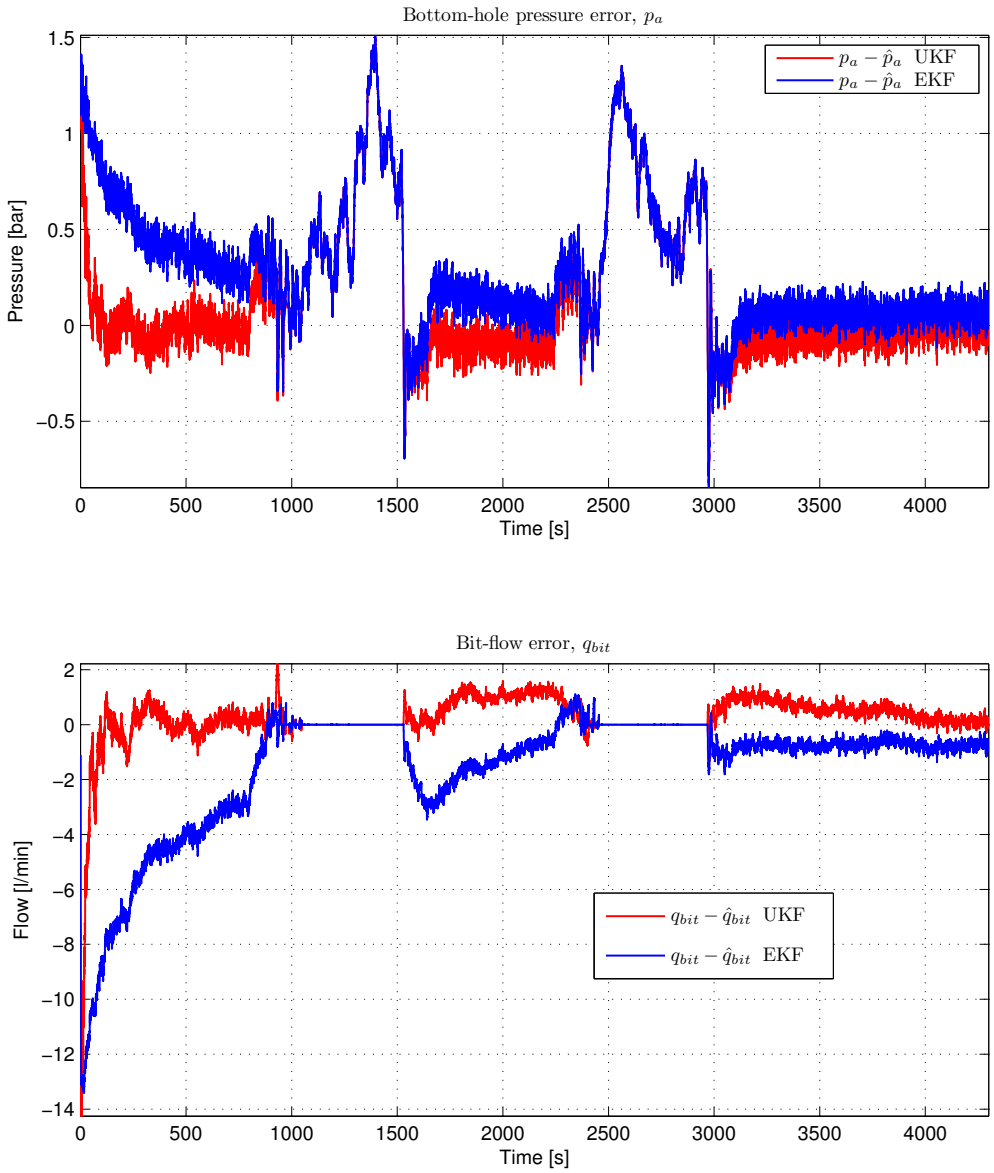

Figure 6.8: Pressure estimation error during pipe-connection. Switching between F_a and β_a

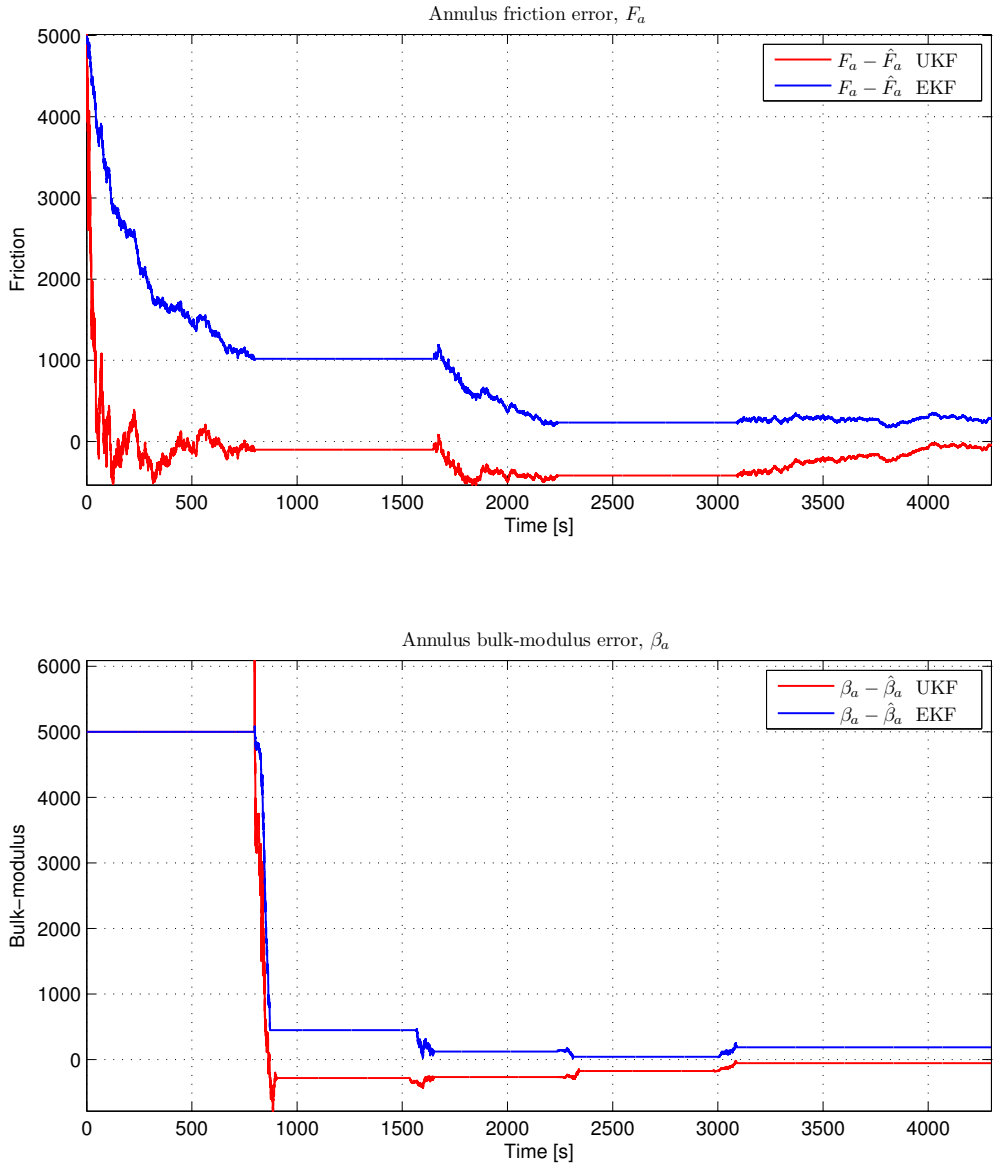

Figure 6.9: Parameter estimation error during pipe-connection. Switching between F_a and β_a

Chapter 7

Wemod simulation

To see how the UKF handles unmodelled dynamics the filter was tested against simulation sets from Wemod. Wemod is a rigid, high-order simulator developed for simulating the flow dynamics in a well. In the simulation scenario; step-responses from mud-pump and a pipe-connection where performed. The influx from the reservoir was set to zero during the simulation.

First the unknown parameters in the process model had to be adapted to Wemod. The parameters ρ_d, ρ_a,F_d and F_a where identified by applying steps in the mud-pump and recording stationary conditions in the pressures p_p, p_c and p_a. These pressures where then utilized to fit the parameters with a least square algorithm according to the stationary equations

$$\begin{aligned} q_{bit} &= q_{pump} \\ p_p - p_c &= (F_d + F_a)q_{bit}^2 - (\rho_d - \rho_a)gh_{bit} \\ p_a - p_c &= F_a q_{bit}^2 + \rho_a g h_{bit} \end{aligned}$$

For the dynamic parameters; β_d, β_a, M_d and M_a; the results given in [11] where utilized. The choke valve was modeled as

$$q_{choke} = C_v \sqrt{\frac{2\Delta p_c}{\rho_a}}$$

where the choke valve constant C_v was calculated according to the stationary equation

$$C_v = \frac{q_{pump} + q_{back}}{\sqrt{2\Delta p_c/\rho_a}}$$

The identified parameters are shown in table 8.1. The pressures are shown in bar and other units follow after this[1]. Figure 7.1 display the pressure and bit-flow progress. The mud-pump is ramped down from 1000 L/min to zero, and at the same time the back-pressure pump is ramped up from 200 L/min

[1] Except for q_{bit}; that for convenience is shown in liter per minute

Parameter	Value
$\bar{\rho}_d$	$1250\,\mathrm{kg/m^3} \cdot 10^{-5}$
$\bar{\rho}_a$	$1250\,\mathrm{kg/m^3} \cdot 10^{-5}$
F_d	$1.676 \cdot 10^5$
F_a	$1.1926 \cdot 10^5$
β_d	13090
β_a	7317
M_d	6064
M_a	1622
V_d	$26.71\,\mathrm{m^3}$
V_a	$99.9\,\mathrm{m^3}$
C_v	$2.819 \cdot 10^{-4}\ h_{bit}\ 2014\,\mathrm{m}$

Table 7.1: Results of fluid model fit to Wemod

to 400 L/min. The Kalman filter estimates the correct stationary values for the bottom-hole pressure, and deviates somewhat during transients. A bit-flow measurement was not available in the Wemod version utilized for simulation[2], but the estimated bit-flow converges to the stationary pump-flow. Figure 7.2 show the estimated pressure deviations, and as mentioned; the bottom-hole pressure has error peaks of up to 15 bar during transients.

Other parameter vectors where also tested against this Wemod scenario. When estimating the choke valve constant and annulus friction during stationary conditions; the valve constant converged to the value in table 8.1. Another parameter vector with β_a and β_d estimated during transients; resulted in β_a converging to zero.

Figure 6.3 shows the estimation of F_a during stationary conditions and β_a during transients. The annulus friction converges to a stationary value whereas β_a does not, is but continuously changed during the simulation. A case where β_a first was estimated from pump excitations; and then halted before the pipe-connection has also been conducted. This gave a larger ISE-value; than continuous estimation of β_a during the mud-pump ramp down.

[2]Version $s01r01$ of Wemod was utilized for simulation

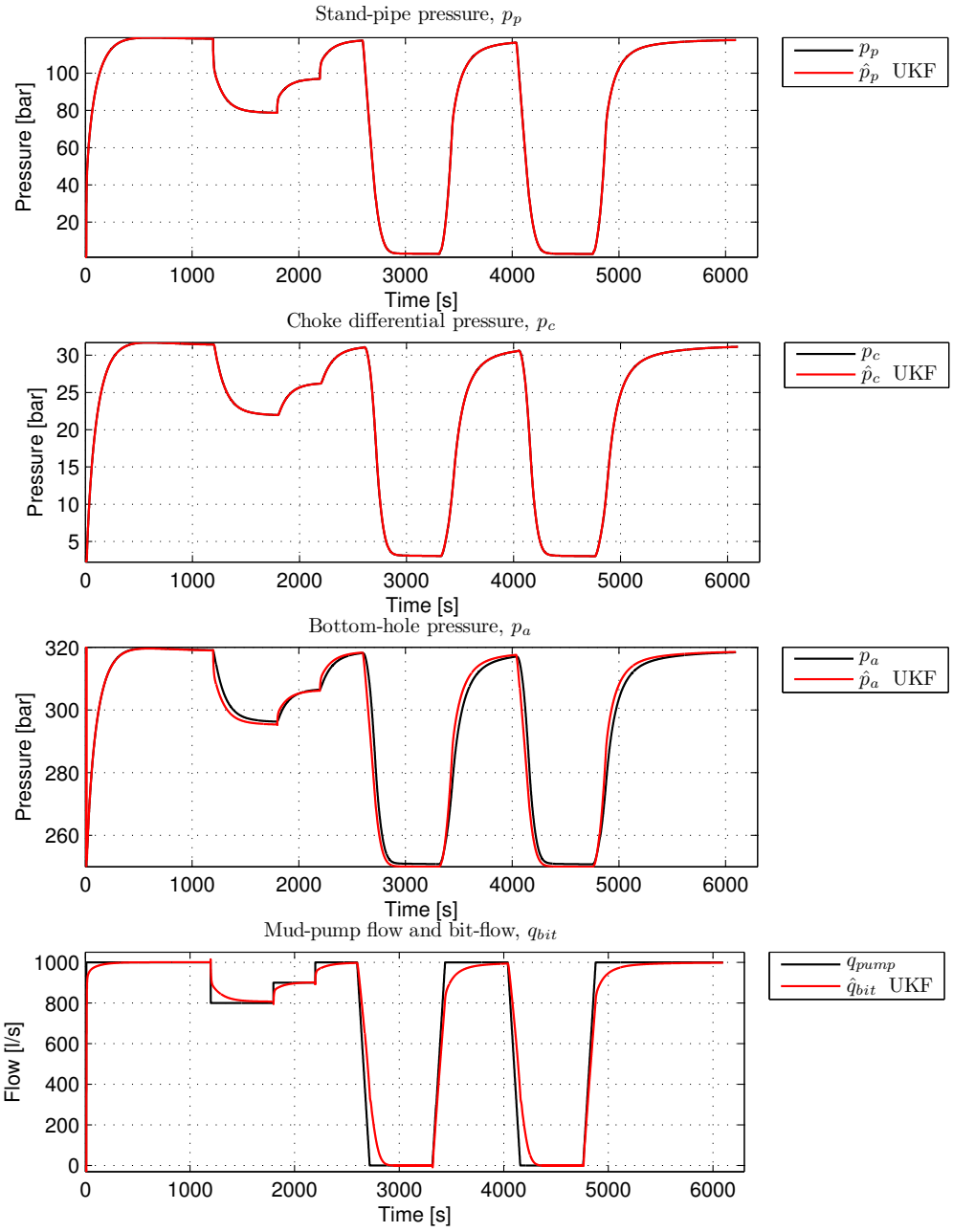

Figure 7.1: Wemod pressure estimates

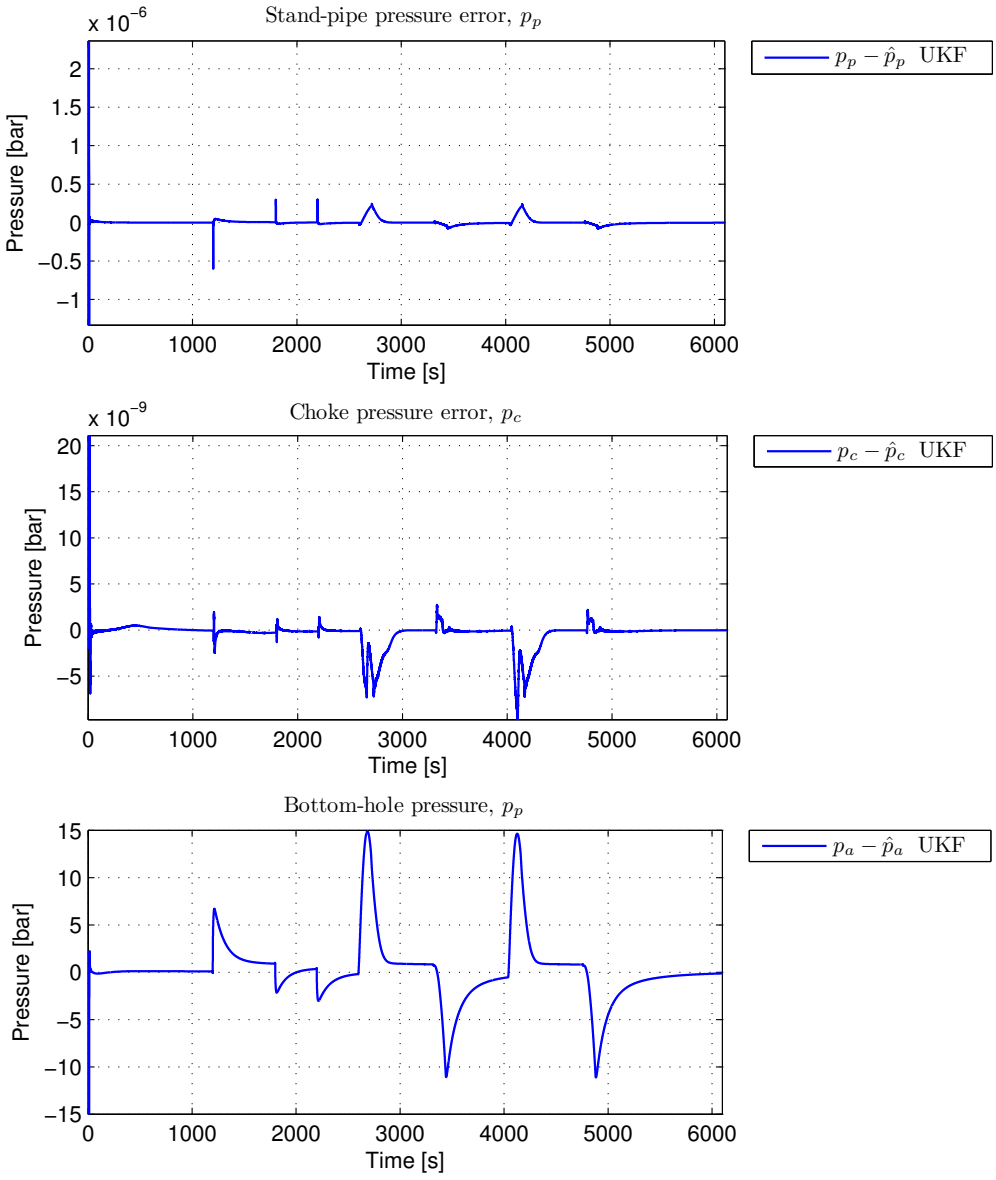

Figure 7.2: Wemod pressure estimate error

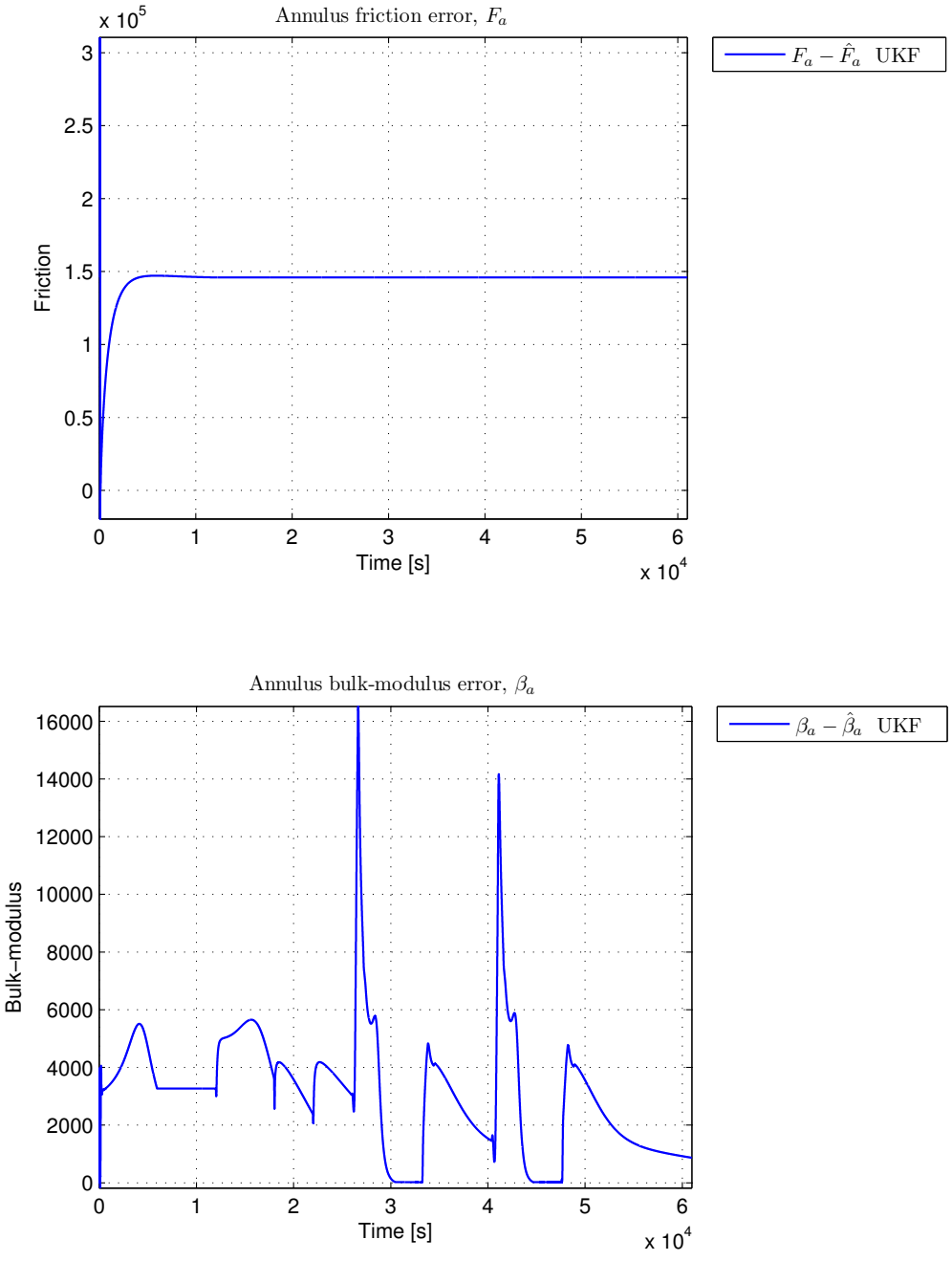

Figure 7.3: Wemod parameter estimates CV, β_a and F_a

Chapter 8

Simulation with data from Grane

8.1 Parameter identification

The observer was tested against a data-set from Grane well G2 Y1. The same data set has also been simulated in [18] against a non-linear adaptive observer. In the simulated data set there was not enough stationary values of q_{pump} to properly estimate all parameters well. Some assumptions about the parameters where therefore made. In the drill-log the mud specific gravity where set to $SG = 1.18$. This gives a fluid density of $\rho_0 = 1.18 \cdot 998 = 1177.6\,\mathrm{kg/m^3}$. In [18]; the average density $\bar{\rho} = 1200\,\mathrm{kg/m^3}$ is applied in the simulation. This is based on the density increase

$$\rho = \rho_0 + \frac{\rho_0}{\beta}(p - p_0)$$

as the well becomes deeper. If we assume that the density in annulus is the same as in the drill-string; the friction can be solved from equations

$$\begin{aligned} q_{bit} &= q_{pump} \\ p_p - p_c &= (F_d + F_a)q_{bit}^2 - (\rho_d - \rho_a)gh_{bit} \\ p_a - p_c &= F_a q_{bit}^2 + \rho_a g h_{bit} \end{aligned}$$

The density term cancels and, this gives enough equations to solve for F_d and F_a. The parameters M_d and M_a where calculated according to equations (3.18). All parameters utilized in the simulations are shown in table 8.1.

There is a large uncertainty combined with the choke flow; q_{choke}. This is partially because the choke characteristic is not exactly known, and also there is an uncertainty in the annulus density. To overcome this problem the valve constant C_v is included in the parameter vector. As already mentioned in section 4.4.1; it is possible to estimate both F_a and C_v during stationary

Parameter	Value
$\bar{\rho}_d$	$1200\ \mathrm{kg/m^3} \cdot 10^{-5}$
$\bar{\rho}_a$	$1200\ \mathrm{kg/m^3} \cdot 10^{-5}$
F_d	$1.4577\ \cdot 10^5$
β_d	14000
β_a	14000
M_d	5998
M_a	1764
V_d	m^3
V_a	$145.11\ \mathrm{m}^3$
h_{bit}	1827 m
l_{bit}	3926 m

Table 8.1: Results of fluid model fit to Wemod

conditions. Since there is some uncertainty combined with the dynamic parameters; β_d, β_a M_d and M_a; the friction and valve constant where only estimated when the filter was stationary. The valve equation utilized in the simulation was derived by Lars Imsland and is displayed in figure The valve

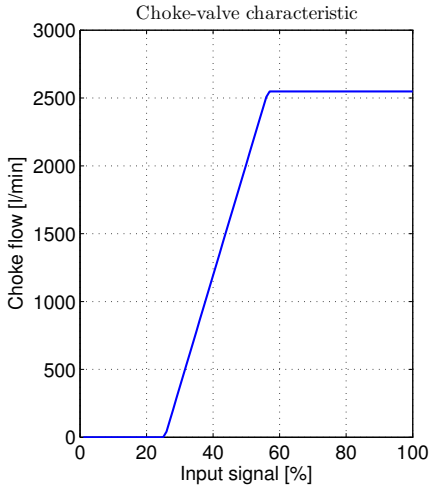

Figure 8.1: Choke-valve characteristic

equation calculates the flow in l/s, and must be converted to m^3/s.

8.2 Grane pipe-connection simulation

The data set was taken from a pipe-connection at Grane well G2 Y1. The measurements utilized in the simulation where

- True vertical depth (TVD), h_{bit}
- Well length, l_{bit}
- Stand-pipe pressure p_p
- Choke differential pressure p_c
- Pump flow q_{pump}
- Choke valve opening u_c

TVD was calculated on-line according to

$$h_{bit} = \frac{BHP \cdot 10^5}{ECD\rho_w g}$$

where ρ_w is water density. The well length was utilized for calculating the annulus and drill-string volumes online. The drill-string length is piecewise constant and during pipe-connections it was extended with 27 meters. This was performed after pump-shut down. Drill-string friction was also recalculated and applied after a pipe-connection. Figure 8.2 display the measured pressures; stand-pipe pressure and choke differential pressure. It also shows the estimated and measured bottom-hole pressure. The last entry in the figure present the estimated bit-flow along with the pump-flow and choke-valve input. The bottom-hole pressure measurement is as mentioned lost when the bit-flow approaches zero. This happens at $t \approx 2300\,\text{s}$ and $t \approx 6800\,\text{s}$. The bottom-hole estimate stays within an error of approximately one bar. Figure 8.3 show the estimated annulus friction and choke-valve constant.

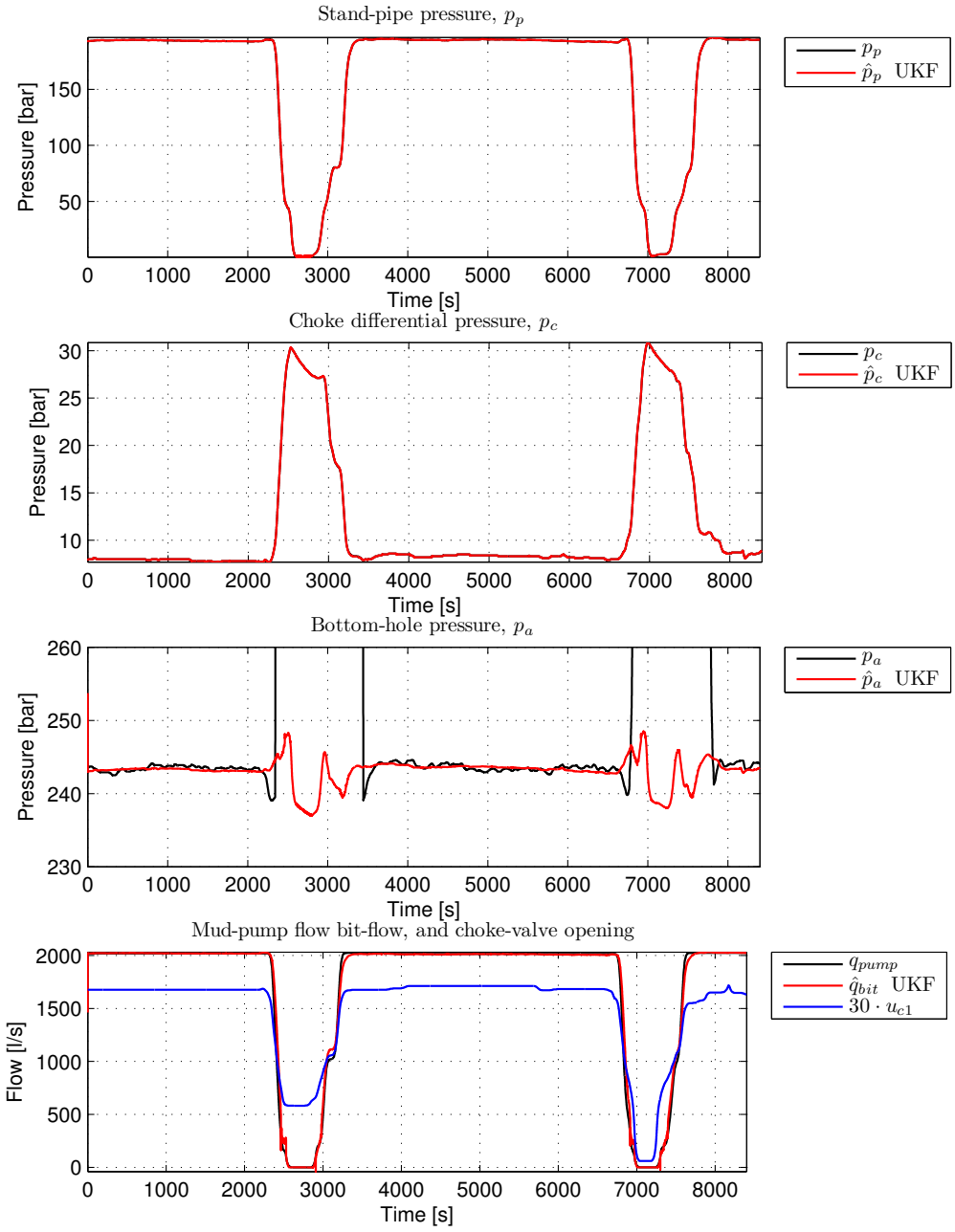

Figure 8.2: Estimated pressures and bit-flow

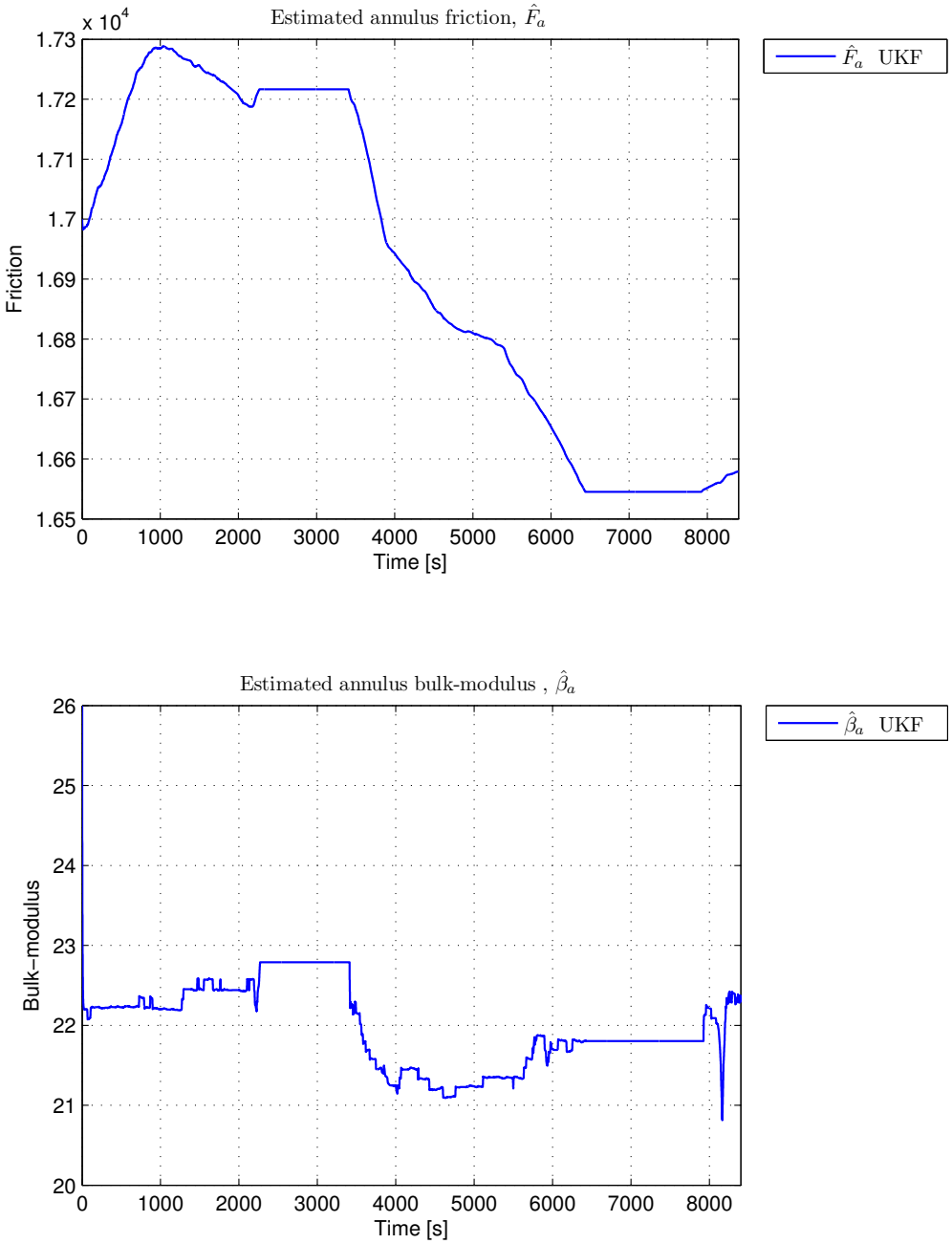

Figure 8.3: Estimated annulus friction and fluid bulk-modulus

Since there is some uncertainty in the parameters estimated off-line; the effect of a larger density in annulus than drill-string was simulated. Instead of identifying F_d off-line; the total friction $F_a + F_d$ was estimated online and annulus friction was set to $F_a = 0.11 \cdot F_d$. The same data set was utilized here as in the simulation described above. Three cases where tested.

1. $F_a = 0.11F_d$ and $\rho_a = \rho_d$
2. $F_a = 0.11F_d$ and $\rho_a = 1.05 \cdot \rho_d$
3. $F_a = 0.11F_d$ and $\rho_a = 1.1 \cdot \rho_d$

In the first case annulus density is equal to drill-string density, and in the second and third case the annulus density is set 5% and 10% larger than the drill-string density. Figure 8.4 shows the bottom-hole pressure measurement and estimate for the three cases. When the annulus density increases the peaks during mud-pump shut down is much larger than when annulus and drill-string density is equal. Figure 8.5 display the friction and choke valve estimates.

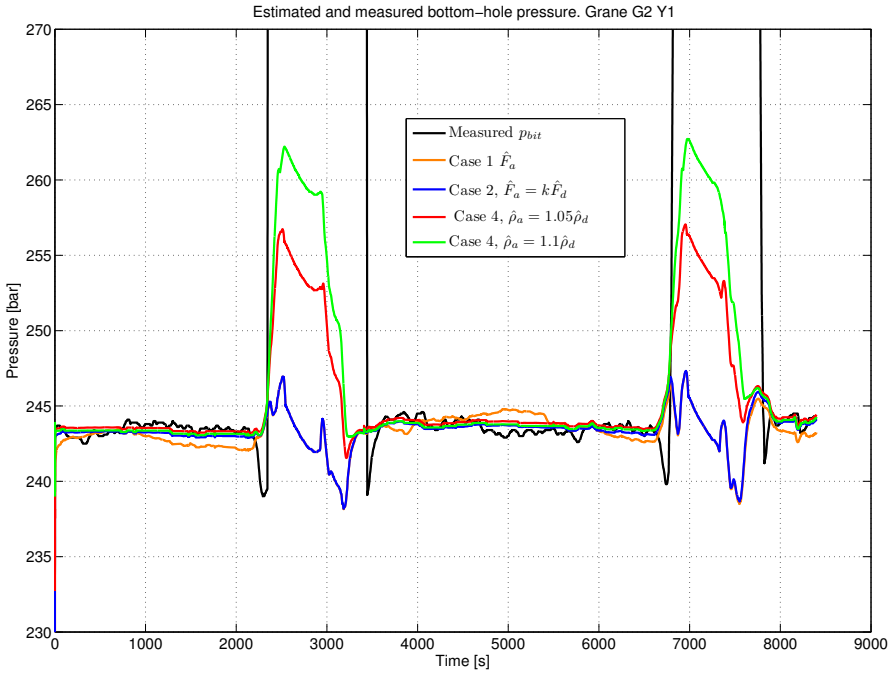

Figure 8.4: Bottom-hole pressure estimate, Grane G2 Y1

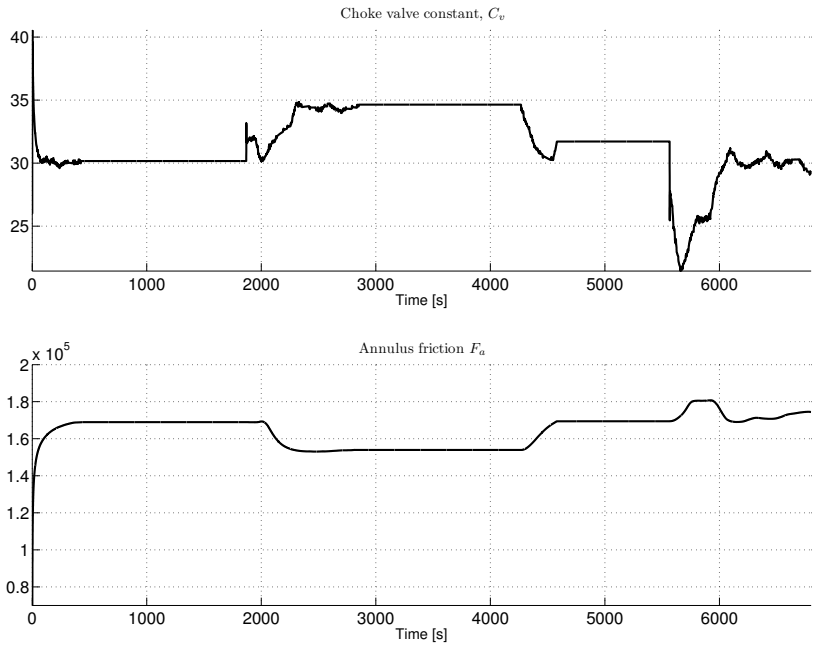

Figure 8.5: Estimated annulus friction and choke valve constant, Grane G2 Y1

Chapter 9

Conclusions

In the observability analysis it was found that the process model is not observable when augmenting the parameter vector with ρ_a, F_a and β_a. To verify this; estimation of the unobservable state vector was simulated. Both filters converged to the correct bottom-hole pressure. The UKF converged to the correct parameter values; whereas the EKF converged to the wrong values. The correct bottom-hole estimate was probably obtained since the bit-flow equation and bottom-hole measurement equation both contains the sum of the estimated parameters; ρ_a and F_a. However; if estimation of these parameters are halted before pump-shut down; the total sum would give the wrong bottom-hole pressure estimate. The process model was also not observable for the parameter vector; ρ_a, F_a and β_a; when the bottom-hole pressure measurement was included. This was also verified in simulations. Since the measurement equation contains all the unknown values for estimating the pressure, the measurement will estimate biased values before the parameters converges. On the other hand; a bottom-hole measurement would add robustness to obtaining the correct parameter values. Based on the observability analysis; the filters where designed to estimate well-bore friction and annulus fluid bulk-modulus. The choke valve constant was also included in the parameter vector for some simulations. Since no more information was gained from the bottom-hole pressure measurement; only the stand-pipe pressure and choke differential pressure where utilized as measurements in the filters.

In the simulations with data generated from the design model; the UKF and EKF where compared. When friction and fluid bulk-modulus in the annulus where estimated; both filters converged to the correct parameter values. The annulus friction was estimated during stationary conditions and fluid bulk-modulus was estimated during transients. Simulations where both parameters where estimated at the same time where also conducted, but they did not give as good results. In the pipe-connection scenario; the filters managed to estimate fluid bulk-modulus during mud-pump shut down.

However; other sources of excitation; such as step-responses from the mud-pump; would be more useful for estimating β.

The UKF had the lowest ISE-value in all simulation scenarios and converged faster to the correct states. It also converged closer to the correct parameter values than the EKF. Based on better performance and easier implementation purposes; w.r.t changing parameters; the UKF was selected for further testing against Wemod and data sets from Grane.

When testing the UKF against data sets from Wemod; different parameter vectors where investigated. Estimation of annulus and drill-string fluid bulk-modulus resulted in β_a converging to zero. This parameter vector was therefore discarded. Estimation of annulus friction during stationary conditions and annulus bulk-modulus during transients gave the lowest ISE-values. The β_a parameter did not converge, but was continuously altered by the filter during simulation. The reason for this could be the effects of model-errors and that the assumed constant parameters where slightly off. The filter estimated the correct stationary values, and had some deviations during transients.

It was also tried to halt the parameter estimation of β_a after a period of excitation from mud-pump. This gave higher ISE-value than when estimating the parameter during all transients. Simulations where the choke valve constant was estimated along with friction was also conducted. In this case the valve constant converged to its correct value.

The UKF was also tested against a data set from the Grane field. The data set consisted of a pipe-connection scenario. Annulus friction and the choke valve constant where estimated during stationary conditions. The filter estimated the bottom-hole pressure within an error difference of 1 bar. The effect of a larger density in annulus than the drill-string was also tested. As expected; this gave much larger peaks during mud-pump shut down than during simulation with equal densities. This shows that it is crucial to have a correct estimate of the annulus density.

Overall the UKF gave promising results in estimating the bottom-hole pressure. The largest concern is the observability problem in estimating annulus density, friction and bulk-modulus. A solution to this problem could be to estimate the densities and friction based on stationary conditions and updating the Kalman filter with these.

9.1 Comments

In the UKF there where some problems where the covariance matrix was not positive definite. In this situation; there may be problems with computing the matrix square root for determining the sigma-points. This was solved by examining the covariance matrix, and if it had negative eigenvalues the covariance matrix from last iteration was utilized instead. Another possibility

is to evaluate the covariance matrix about $\mathcal{X}_{k+1|k}$. The UKF did not handle the situation where $q_{bit} \rightarrow 0$ to well. Since the UKF calculates sigma-points based on the covariance and process noise covariance matrix; this was actually solved by decreasing the process noise covariance during low bit-flows. Also, careful tuning of the covariance matrices is important in obtaining the correct estimates. If the covariance matrix is not properly tuned; the filter may estimate wrong parameter values.

9.2 Future work

The annulus density and bore-hole friction are two very important parameters when estimating the bottom-hole pressure. The possibility of designing an observer for both of these parameters should therefore be investigated. One possibility is to see if the Kalman filter is able to estimate the correct values during excitation. Here; the effect of an error in the fluid compressibility should also be tested. Another way is to implement a recursive least square algorithm based on stationary pressures and pump-flows. This also requires knowing exactly when the process is stationary and a method for transient detection should be implemented.

There are some problems with numerically stability during low bit-flows. A solution for this problem might be to utilize a different solver. An implicit solver with fixed step size that is stable for the hole left half-plane can be implemented. The problem could also be solved by modifying the choke valve equation during low flows.

There are also more simulations that must be conducted. Simulation against real data sets with bottom-hole measurements must be examined to see if the observer estimates the correct values during pipe-connection. Transients may also be utilized for bulk-modulus estimation and this must be tested against real data. An important variable not considered here is influx from the reservoir. The UKF should be implemented and tested with influx as an estimated parameter.

Other versions of the UKF might be advantageous and should be considered. The square root unscented Kalman filter (SRUKF) ensures numerical stability and guarantee a positive definite covariance matrix. The SRUKF can also be implemented to run at a computational complexity of $\mathcal{O}(n^2)$ when utilized for parameter estimation. This could be accomplished by implementing a dual-UKF; where the states are estimated in one filter and the parameters in another filter. In comparison; the EKF has a computational complexity of $\mathcal{O}(n^2)$ for parameter estimation; whereas the UKF has $\mathcal{O}(n^3)$ for the same problem.

Appendix A

Kalman filter algorithms

Let the nonlinear state and measurement equations be given by

$$\begin{aligned} x_{k+1} &= f(x_k, u_k) + hw_k \\ y_k &= h(x_k, u_k) + hv_k \end{aligned}$$

where x_k represents the states, u_k are inputs, w_k is process noise and v_k is measurement noise.

A.1 EKF algorithm

Initialization

$$\begin{aligned} \hat{x}_0 &= E[x_0] \\ P_{x,0} &= E[(x_0 - \hat{x}_0)(x_0 - \hat{x}_0)^T] \\ Q &= E[(w_0 - \hat{w}_0)(w_0 - \hat{w}_0)^T] \\ R &= E[(v_0 - \hat{v}_0)(v_0 - \hat{v}_0)^T] \end{aligned}$$

For $k \in \{1, 2, \ldots, \infty\}$ repeat steps 1 to 5

1. Determine measurement model Jacobian's

$$H_{x_k} = \nabla_x \, h(x, u_k, w_k)|_{x=\hat{x}_k^-}$$

2. Compute Kalman gain and filtrate states and covariance

$$\begin{aligned} K_k &= P_{x_k}^- H_{x_k}^T (H_{x_k} P_{x_k} H_{x_k}^T + Q) \\ \hat{x}_k &= \hat{x}_k^- + K_k(y_k - h(\hat{x}_k^-)) \\ P_{x_k} &= (I - K_k H_{x_k}) P_{x_k}^- (I - K_k H_{x_k})^T + K_k R K_k^T \end{aligned}$$

3. Compute process model Jacobian's

$$F_{x_k} = \nabla_x \, f(x, u_k, w_k)|_{x_k = \hat{x}_k^-}$$

4. Calculate time update for process states and covariance

$$\hat{x}_k^- = f(\hat{x}_k, u_k)$$
$$P_{x_k}^- = F_{x_k} P_{x_k} F_{x_k}^T + R$$

5. Check constraints

A.2 UKF algorithm

Initialization:

$$\hat{\mathbf{x}}_\mathbf{0} = E[\mathbf{x_0}]$$
$$\mathbf{P_0} = E[(\mathbf{x_0} - \hat{\mathbf{x}}_\mathbf{0})(\mathbf{x_0} - \hat{\mathbf{x}}_\mathbf{0})^T]$$
$$\mathbf{x_0^a} = \begin{pmatrix} \hat{\mathbf{x}}_\mathbf{0} & \mathbf{0} & \mathbf{0} \end{pmatrix}^T$$
$$\mathbf{P_0^a} = E[(\mathbf{x_0^a} - \hat{\mathbf{x}}_\mathbf{0}^\mathbf{a})(\mathbf{x_0^a} - \hat{\mathbf{x}}_\mathbf{0}^\mathbf{a})^T] = \begin{pmatrix} \mathbf{P_0} & \mathbf{0} & \mathbf{0} \\ \mathbf{0} & \mathbf{Q} & \mathbf{0} \\ \mathbf{0} & \mathbf{0} & \mathbf{R} \end{pmatrix}$$

For $k \in \{1, 2, \ldots, \infty\}$ repeat steps 1 to 9

1. Calculate sigma-points

$$\mathcal{X}_{k-1}^a = \begin{pmatrix} \hat{\mathbf{x}}_\mathbf{k-1}^\mathbf{a} & \hat{\mathbf{x}}_\mathbf{k-1}^\mathbf{a} \pm \sqrt{(N+\lambda)\mathbf{P}_\mathbf{k-1}^\mathbf{a}} \end{pmatrix}$$

2. Time update for state equations

$$\mathcal{X}_{k|k-1}^x = \mathbf{f}(\mathcal{X}_{k-1}^x, \mathcal{X}_{k-1}^w)$$

3. Check state constraints

$$\mathcal{X}_{k|k-1}^x = \begin{cases} \mathcal{X}_{k|k-1}^x & \text{if } \mathcal{X}_{k|k-1}^x < b \\ b & \text{if } \mathcal{X}_{k|k-1}^x \geq b \end{cases}$$

4. Determine state output mean and state output covariance

$$\hat{\mathbf{x}}_\mathbf{k}^- = \sum_{i=0}^{2N} W_i^{(m)} \mathcal{X}_{i,k|k-1}^x$$
$$\mathbf{P}_\mathbf{k}^- = \sum_{i=0}^{2N} W_i^{(c)} (\mathcal{X}_{i,k|k-1}^x - \hat{x}_k^-)(\mathcal{X}_{i,k|k-1}^x - \hat{x}_k^-)^T$$

5. Time update for measurement equations

$$\mathcal{Y}_{k|k-1} = \mathbf{h}(\mathcal{X}^x_{k-1}, \mathcal{X}^v_{k-1})$$

6. Check constraints

$$\mathcal{Y}_{k|k-1} = \begin{cases} \mathcal{Y}_{k|k-1} & \text{if } \mathcal{Y}_{k|k-1} < c \\ b & \text{if } \mathcal{Y}_{k|k-1} \geq c \end{cases}$$

7. Measurement output mean and covariance

$$\hat{\mathbf{y}}^-_{\mathbf{k}} = \sum_{i=0}^{2N} W_i^{(m)} \mathcal{Y}^x_{i,k|k-1}$$
$$\mathbf{P}_{\bar{\mathbf{y}}_{\mathbf{k}}\bar{\mathbf{y}}_{\mathbf{k}}} = \sum_{i=0}^{2N} W_i^{(c)} (\mathcal{Y}^x_{i,k|k-1} - \hat{y}^-_k)(\mathcal{Y}^x_{i,k|k-1} - \hat{y}^-_k)^T$$

8. Compute measurement and state cross covariance

$$\mathbf{P}_{\mathbf{x}_{\mathbf{k}}\mathbf{y}_{\mathbf{k}}} = \sum_{i=0}^{2N} W_i^{(c)} (\mathcal{X}^x_{i,k|k-1} - \hat{x}^-_k)(\mathcal{Y}^x_{i,k|k-1} - \hat{y}^-_k)^T$$

9. Calculate Kalman gain and filtrate filtrate

$$\mathbf{K}_{\mathbf{k}} = \mathbf{P}_{\mathbf{x}_{\mathbf{k}}\mathbf{y}_{\mathbf{k}}} {\mathbf{P}_{\bar{\mathbf{y}}\bar{\mathbf{y}}}}^{-1}$$
$$\hat{\mathbf{x}}_{\mathbf{k}} = \hat{\mathbf{x}}^-_{\mathbf{k}} + \mathbf{K}_{\mathbf{k}}(\mathbf{y}_{\mathbf{k}} - \hat{\mathbf{y}}^-_{\mathbf{k}})$$
$$\mathbf{P}_{\mathbf{k}} = \mathbf{P}^-_{\mathbf{k}} + K_k \mathbf{P}_{\bar{\mathbf{y}}\bar{\mathbf{y}}} K_k^T$$

Appendix B

Jacobian for parameter vector $\theta = (\rho_a \;\; F_a \;\; \beta_a)$

$$\mathbf{F} = \frac{\partial \mathbf{f}}{\partial \mathbf{x}} = \begin{pmatrix} 0 & 0 & -\frac{\beta_d}{V_d} & 0 & 0 & 0 \\ 0 & \frac{\partial f_2}{\partial p_c} & \frac{\beta_a}{V_a} & \frac{\partial f_2}{\partial \rho_a} & 0 & \frac{\partial f_2}{\partial \beta_a} \\ \frac{1}{M_a+M_d} & \frac{-1}{M_a+M_d} & \frac{\partial f_3}{\partial q_{bit}} & \frac{-gh_{bit}}{M_a+M_d} & \frac{-(q_{bit}-q_{res})^2}{M_a+M_d} & 0 \\ 0 & 0 & 0 & 1 & 0 & 0 \\ 0 & 0 & 0 & 0 & 1 & 0 \\ 0 & 0 & 0 & 0 & 0 & 1 \end{pmatrix} \tag{B.1}$$

$$\begin{aligned} \frac{\partial f_2}{\partial p_c} &= -\frac{1}{2}\frac{\beta_a z A_c K_c \sqrt{2}}{\sqrt{\frac{p_c-p_0}{\rho_{a0}}\rho_{a0} V_a}} \\ \frac{\partial f_2}{\partial \rho_a} &= \frac{1}{2}\frac{\beta_a z K_c \sqrt{2}(p_c-p_0)}{\sqrt{\frac{p_c-p_0}{\rho_a}\rho_a^2 V_a}} \\ \frac{\partial f_2}{\partial \beta_a} &= \frac{1}{V_a}\left(-V_a + q_{bit} + q_{res} + q_{back} - z K_c \sqrt{2}\sqrt{\frac{(p_c-p_0)}{\rho_a}}\right) \\ \frac{\partial f_3}{\partial q_{bit}} &= \frac{-2F_d q_{bit} - 2F_a(q_{bit}-q_{res})}{M_d + M_a} \end{aligned} \tag{B.2}$$

Bibliography

[1] Rambabu Kandepu Bjarne Foss Lars Imsland. Applying the unscented kalman filter for nonlinear state estimation. *Journal of process control*, 2007.

[2] M. Oussalah De Schutter. Adaptive kalman filter for noise identification.

[3] K. Xiong H.Y. Zhang C.W Chan. Performance evaluation of ukf-based nonlinear filtering. *automatica*, 2004.

[4] Olav Egeland Jan Tommy Gravdahl. *Modeling and simulation for automatic control.* Marine Cybernetics, 2003.

[5] Simon J. Julier Jeffrey K. Uhlmann. A new extension of the kalman filter to nonlinear systems. Technical report, Department of Engineering Science, The University of Oxford, 1997.

[6] Robert Grover Brown Patrick Y. C. Hwang. *Introduction to random signals and applied kalman filtering.* Wiley, 1997.

[7] Eric A. Wan Rudolph van der Merwe. The unscented kalman filter for nonlinear estimation. Technical report, Oregon Graduate Institute of Science and Technology, 2001.

[8] Pierre R. Bélanger. Estimation of noise covariance matrices for a linear time-varying stochastic process. *Automatica*, 1974.

[9] Chi-Tsong Chen. *Linear system theory and design.* Oxford university press, 1999.

[10] Rolf Henriksen. Stokastiske systemer. Technical report, Institutt for teknisk kybernetikk, Gløshaugen, 1998.

[11] Lars Imsland. Mpd estimation. Technical report, Sintef, 2008.

[12] Glenn-Ole Kaasa. A simpe dynamic model of drilling for control... Technical report, Hydro oil and energy, Research centre in Porsgrunn, 2007.

[13] Frank L. Lewis. *Optimal estimation.* Wiley, 1986.

[14] Raman K. Mehra. Identification of variances and adaptive kalman filtering. *IEEE Transactions on automatic control*, 1970.

[15] Reid G. Reynolds. Robust estimation of covariance matrices. *Identification of variances and adaptive Kalman filtering*, 1990.

[16] Thomas Rognmo. Performance and robustness-analysis of mpd control. Technical report, NTNU, 2007.

[17] Øyvind Breyholtz. Linear model predictive pressure control during drilling operations. Technical report, NTNU, 2007.

[18] Øyvind Nistad Stamnes. Adaptive observer for bottomhole pressure during drilling. Master's thesis, NTNU, 2007.